[redacted]

[redacted]

[redacted]

GENERAL DYNAMICS

Convair Division

A2136-1 (REV. 5-65)

CENTAUR AC-8

POSTFLIGHT GUIDANCE

ANALYSIS

GDC-BTD66-072
1 JULY 1966

N. Strano, Lewis Proj. Mgr.

Prepared by: J. Greenstein
J. Greenstein

L. Ojeda
L. Ojeda

R. Wagar
R. Wagar

M. Winkler
M. Winkler

Checked by: J. Greenstein
J. Greenstein
Design Specialist
Inertial Guidance

Approved by:
R. P. Day
Group Engineer
Inertial Guidance

Approved by:
R. S. Wentink
Asst. Chief Engineer
Design Analysis - LVP

GENERAL DYNAMICS
Convair Division

FOREWORD

This report presents a postflight performance analysis of the AC-8 guidance equations and guidance system (MGS 30). The AC-8 vehicle was launched on 7 April 1966 from ETR Complex 36B. This analysis and documentation was performed in compliance with Item 64 of the Centaur Documentation Requirements Plan (Contract NAS 3-8701).

SUMMARY

Flight Description. The AC-8 was launched from ETR Complex 36B on 7 April 1966 and was to fly a two-burn trajectory into a simulated lunar transfer orbit. The first burn was successful. Compared to the nominal trajectory, BECO occurred 0.4 second early, SECO occurred 7.9 seconds early, and MECO occurred 1.9 seconds late.

Analysis of the energy at first MECO indicates an 11 millisecond cutoff extrapolation error. This caused a -0.7 ft/sec velocity error at cutoff. The parking orbit perigee altitude was 89.0 n.mi. compared to the nominal value of 89.9 n.mi. After the 25 minute coast period, second MES was not successful because of H_2O_2 depletion.

Computer Performance. The guidance computer appeared to operate flawlessly until 2,290 seconds, the end of telemetry coverage. All expected guidance discretes were issued and equation branching occurred as expected. Analysis of the sigmator operation indicated no significant sigmator errors.

Velocity Comparison. A comparison between the ETR BET and telemetered guidance trajectory data gave thrust velocity errors of -0.5 ft/sec, -3.3 ft/sec and -4.2 ft/sec for the u, v, and w components respectively. This compares with 6.5 ft/sec, -1.5 ft/sec, and 12 ft/sec for AC-6 at the corresponding time of flight.

Error Separation. Analysis of the velocity data during the coast period indicated very small accelerometer bias errors. The errors derived were 22 μg, 22 μg, and -59 μg for the u, v, and w accelerometers re- respectively; which compares with the 04040 specification of 300, 480, and 480 μg.

Telemetered gimbal motor demodulator outputs indicate an average platform pitch error of approximately 7 arc seconds.

After removing the above errors from the velocity residuals, the following errors were indicated.

u accelerometer scale factor, -0.004%

v accelerometer misalignment with respect to the u axis, -35 arc seconds

v gyro MUIA drift, 0.10 deg/hr/g

SUMMARY, Contd.

Guidance Steering Analysis. The steering loop kept the vehicle thrust vector closely aligned with the velocity-to-be-gained vector. No significant resolver chain errors were indicated by the integral control term.

The altitude control term was successful in achieving an insertion altitude within the software specification of 3.5 n.mi. The guidance computed insertion altitude was approximately 1 n.mi. low.

The yaw steering equations successfully removed the yaw velocity error.

Accelerometer Limit Cycle Analysis. The accelerometers exhibited fewer different limit cycles than any previous flight. Most time intervals exhibited 3/2, 2/2, and 2/3 limit cycles only.

Analog Measurements. The only problem indicated by the analog guidance data was an unexplained shift of 0.9 deg/hr on the w component of gyro torquing. This would have caused an error of 12 ft/sec on the v velocity component. No large error of this magnitude showed up, therefore the error appears to be due to telemetry instrumentation.

Calibration Data. A statistical analysis of the calibration shift data for MGS 30 indicated the standard deviation of shifts were well within specification. The new GG 177 accelerometers exhibited much smaller scale factor shifts. For example the standard deviation of shifts were approximately one-half the value observed on the AC-6 system.

TABLE OF CONTENTS

TABLE OF CONTENTS (Contd)

LIST OF ILLUSTRATIONS

LIST OF ILLUSTRATIONS (Contd)

LIST OF TABLES

SECTION 1

INTRODUCTION

The AC-8 vehicle was launched from ETR Complex 36B on 7 April 1966. It carried a 1730-pound mass model of the Surveyor payload and was designed to demonstrate a two-burn mission capability. The AC-8 also contained an uprated guidance system: a Phase I PIP system with GG177 accelerometers.

The guidance flight test objectives were to:

a. Demonstrate the system integrity of the uprated guidance system.

b. Demonstrate that the guidance system provides proper discrete and steering signals to the Atlas and Centaur flight control systems.

c. Demonstrate the parking orbit, the guidance equations, and associated trajectory parameters of a two-burn mission.

d. Obtain data on the measuring accuracy of the guidance system.

All of the first-burn and coast guidance objectives were met. The Centaur was inserted into an approximately 90 n.mi. circular orbit as planned. Second MES was not successful because of H_2O_2 depletion. At second MES the C2 engine ignited for a brief period, causing the vehicle to undergo a severe tumbling and rolling motion.

An analysis of the performance of the guidance equations and guidance hardware is presented in this report. The analysis is primarily based upon the telemetered digital computer and Δv pulse data. Detailed analysis of the telemetered analog guidance data, as well as other flight systems, are presented in GDC-BNZ66-026, Atlas/Centaur Flight Evaluation Report, AC-8.

Performance of the computer operations is presented in Section 2. A comparison of the nominal and actual trajectory, cutoff parameters, and flight sequence of events is given in Section 3. An analysis of the performance of the steering equations is given in Section 4. A comparison of the guidance trajectory determined from digital telemetry data with the ETR Best Estimated Trajectory (BET) is given in Section 5. Results of the guidance error separation based upon the BET trajectory is given in Section 6. Accelerometer limit cycle analysis is given in Section 7.

A brief discussion of the analog measurements obtained during the flight is given in Section 8. The guidance telemetry coverage is given in Section 9. Preflight calibration data and a statistical analysis of the calibration shifts are presented in Section 10. The guidance equations and guidance constants used on the AC-8 flight are given in the Appendix.

SECTION 2

COMPUTER OPERATION

2.1 SIGMATOR PERFORMANCE. The vehicleborne Kearfott computer sigmator sums the accelerometer pulses to form velocity; it then sums the sigmator velocity to form position. An IBM 7094 program, SPAT, was used to check the sigmator operation out to 800 seconds. SPAT accumulates the telemetered pulses to form velocity 200 times per second, using a count of the pulses as a time standard. The velocity determined by the simulation agreed with the sigmator value within 0.3 ft/sec. The difference is in part due to the SPAT program timing adjustments which are limited to 0.005 second. The program, therefore, cannot exactly simulate the speed of the vehicleborne computer drum.

Another IBM 7094 program was used to check the sigmator positions. This program integrates the telemetered sigmator velocities using a second-degree numerical integration and differences this position with the telemetered sigmator position. Telemetered and simulation position differences are shown below.

DIRECTION	1ST MECO (ft)	2017 SEC (ft)
u	108	123
v	22	73
w	42	62

These differences are not significant.

2.2 COMPUTATION CHECK. A guidance computer interpretive simulation was used to check the guidance computer calculations. The interpretive simulation is an IBM 7094 computer program designed to duplicate exactly the guidance computer computations, commands, and telemetry when given the basic inputs to the computation cycle. The basic inputs (available from telemetry) are time (T), sigmator velocity ($\bar{v}_\sigma$), and sigmator position ($\bar{r}_\sigma$).

The resulting outputs ($\bar{r}_m$, $\bar{v}_m$, $\bar{\omega}_d$, $\bar{f}^*$, ϵ_a, ϵ, Δt_{co}, ϕ, Code Word) were compared bit-for-bit with the telemetered inflight-computed quantities. Except for periods of data dropout occurring at computer times 1665, 1840, and 1847 seconds, no differences were found throughout the period of continuous telemetry coverage (T = 0 to 2290 seconds). Careful engineering examination of the simulation outputs during the three periods of telemetry dropout lead to the conclusion that the differences observed at these times were due to incorrect processing of the telemetered data. Hence, this bit-for-bit simulation illustrates that the arithmetic and memory functions of the guidance computer performed flawlessly.

SECTION 3

TRAJECTORY COMPARISON

The purpose of the AC-8 mission was to fly a two-burn trajectory into a simulated lunar transfer orbit. The target point was 380,000 km from the earth's center.

The AC-8 equations were coded with launch-on-time capability, although the mission objectives did not call for a demonstration of this capability. Since launch-on-time was not to be demonstrated, a single trajectory was targeted to simulate a lunar launch at 5 hours, 1 minute (GMT) on 26 April 1966. All launch-time dependent terms in the polynominals were set to zero (except the constant term).

The following trajectory constraints were applied to the nominal trajectory:[1]

a. A launch from Complex 36-B (u axis aligned to 115 degrees east of north) and vehicle roll to 103 degrees east of north.

b. Nominal 90-n.mi. parking orbit altitude after first MECO.

c. Parking orbit coast time of 25 minutes.

d. Second-burn injection vis-viva energy integral of -0.85 km^2/sec^2.

e. Injection true anomaly of approximately 4.4 degrees.

3.1 ACTUAL VERSUS NOMINAL TRAJECTORY. A comparison of the actual trajectory during first burn, based upon the ETR BET (Best Estimated Trajectory), with the nominal trajectory is shown in Figure 3-1. It is apparent that during this portion of the flight, the actual trajectory closely followed the preflight-predicted nominal. After the 25-minute parking orbit coast, second MES was not successful because of H_2O_2 depletion. The C2 engine fired for a brief period causing the vehicle to undergo a severe rolling and tumbling motion.

Nominal versus BET position and velocity data are compared at BECO, SECO, and first MECO in Table 3-1. All times are referenced to 2-inch motion. At BECO the flight was close to nominal. It was slightly lower and further down range than nominal, and the velocity was slightly faster than nominal. SECO occurred 7.973 seconds earlier than nominal and was caused by fuel depletion rather than the planned LO_2 depletion. Earlier than expected SECO caused a trajectory dispersion, as is evident

[1] Final Guidance Equations and Performance Analysis for Centaur AC-8, GDC-BTD65-178, 22 January 1966

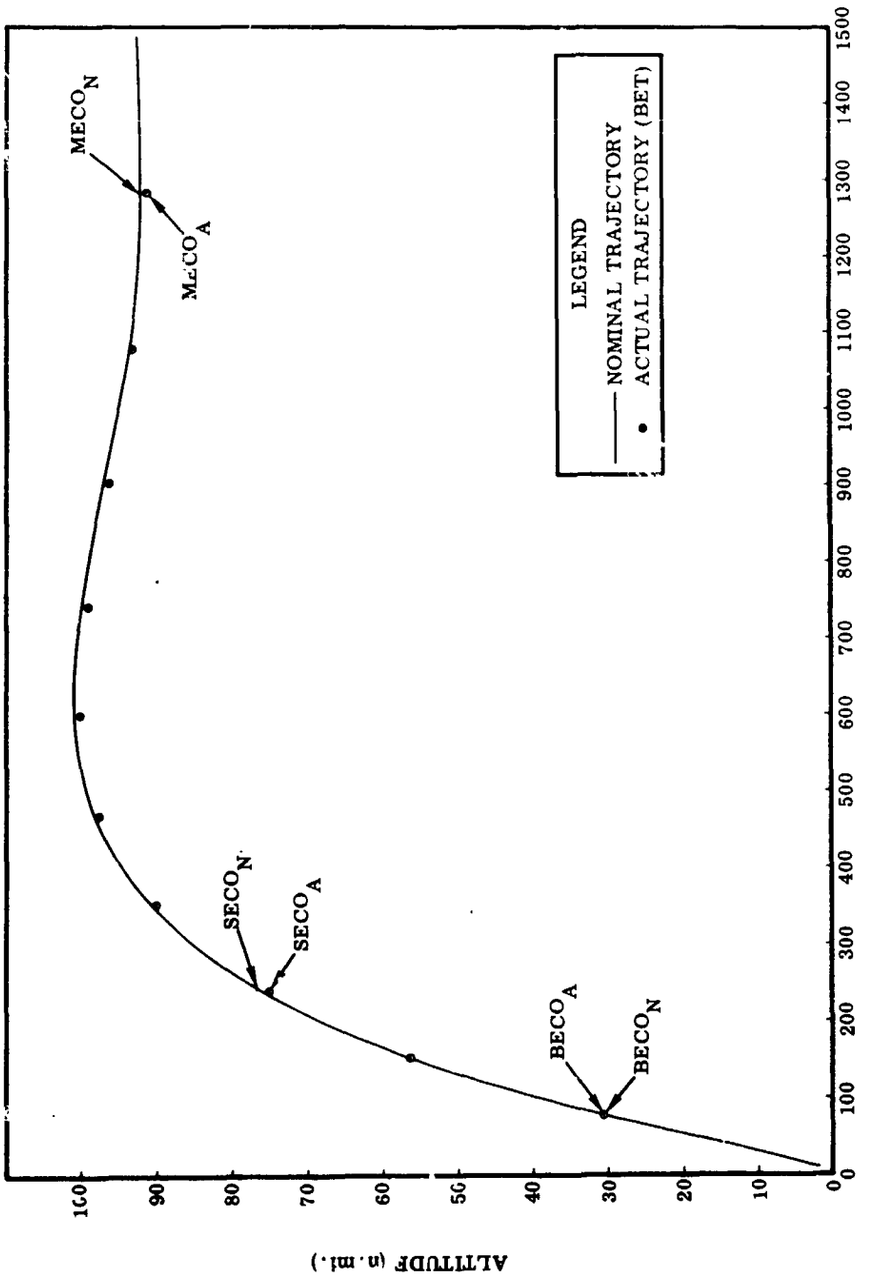

Figure 3-1. AC-8 Nominal and Flight Trajectory Profile

Table 3-1. AC-8 Flight and Nominal Trajectory Comparison

POSITION

EVENT (sec)	$\bar{r}_B$ (uvw) (ft)	$\bar{r}_N$ (uvw) (ft)	$\Delta\bar{r}$ (uvw) (ft)	r_B MAG (ft)	r_N MAG (ft)	Δr MAG (ft)
BECO	475,221.8	471,733.6	3488.2			
T_B = 142.214	90,079.7	90,126.6	-46.9	21,100,751.0	21,102,393.0	- 1,642
T_N = 142.630	21,095,207.0	21,096,927.0	-1720.0			
SECO	1,377,465.1	1,454,383.4	-76,918.3			
T_B = 229.460	304,694.2	327,746.1	-23,051.9	21,349,406.0	21,368,394.0	-18,888
T_N = 237.353	21,302,745.0	21,316,323.0	-13,578.0			
MECO	7,222,490.0	7,177,605.5	44,884.5			
T_B = 575.455	1,631,225.3	1,628,795.4	2,429.9	21,466,445.0	21,471,683.0	- 5,238
T_N = 573.537	20,149,041.0	20,170,825.0	-21,784.			

VELOCITY

EVENT (sec)	$\bar{v}_B$ (uvw) (ft/sec)	$\bar{v}_N$ (uvw) (ft/sec)	$\Delta\bar{v}$ (uvw) (ft/sec)	v_B MAG (ft/sec)	v_N MAG (ft/sec)	Δv MAG (ft/sec)
BECO	8,639.3	8,561.8	77.5			
T_B = 142.214	2,119.5	2,161.5	-42.0	9,465.4	9,413.2	52.2
T_N = 142.630	3,234.7	3,260.5	-25.8			
SECO						
T_B = 229.460	12,302.3	12,501.7	-199.4			
T_N = 237.353	2,854.4	2,920.3	-65.9	12,717.5	12,908.4	-190.9
	1,496.5	1,344.1	152.4			
MECO	23. 47.2	23,459.7	-12.5			
T_B = 575.455	5,279.5	5,279.4	0.1	25,604.1	25,597.7	6.4
T_N = 573.537	-8,827.5	-8,775.6	-51.9			

Time is referenced from 2-inch motion T = 0.

B: BET

N: Nominal

by the differences in position and velocity at SECO. However, the dispersion was handled very well by the guidance equations so that by first MECO the trajectory was only 5238 feet lower and 6.4 ft/sec faster than nominal. Since the MECO criterion is orbital energy, a higher cutoff velocity results when the injection altitude is lower.

Further evidence that the SECO dispersion was corrected by the guidance equations is presented in Table 3-2. This table presents nominal, guidance, and actual parking orbit parameters after VECO. The guidance orbital parameters (GET) were based upon telemetered computer data corrected for inflight software approximations. The "actual" orbital parameters are based upon the BET, although the BET was too noisy at this point to use directly. The actual parameters were therefore determined by adding to the guidance-derived position and velocity vectors:

a. GET-BET velocity errors at MECO

b. GET-BET position errors extrapolated from MECO to 680 seconds

The guidance-nominal coast perigee deviation of -1.03 n.mi. is well within the software specification of 3.5 n.mi. The close comparison of the guidance and actual orbital data is an indication of small guidance hardware errors.

3.2 GUIDANCE PROGRAMMED SEQUENCE OF EVENTS. The guidance equations are responsible for initiating various autopilot and engine sequences. An analysis of the flight sequence of events indicates that all guidance discretes were issued. All guidance equation logical tests and equation branching occurred as expected.

The programmed sequence of flight events that pertain to guidance and equation branching are presented in Table 3-3. Brief descriptions of each event are included. Those events representing changes in the telemetered code word are indicated by asterisks. A code word modification, performed as a result of passing a particular equation test in the i^{th} compute cycle, does not appear in telemetry until the i + 1 compute cycle. The times shown in Table 3-3 represent the telemetered computer time from the compute cycle when the indicated equation test was passed; they do not represent the time of telemetering the modified code word.

The major events are discussed below.

BECO. BECO was commanded by the guidance L3 discrete approximately 7.2 seconds after autopilot BECO enable. The BECO backup (Atlas accelerometer) was not used. The cutoff parameter for BECO is $a_T^2 > 30,982.0$ $(ft/sec^2)^2$, and this test on a_T^2 was passed during the compute cycle beginning at computer time 149.675 seconds. The BECO discrete (L3) was actually issued by the guidance equations at 150.566 seconds. At the time the engine began shutting down, $a_T^2 = 33,600$ $(ft/sec^2)^2$ and $a_T = 183.3$ ft/sec^2 which corresponds to 5.697 g's. This compares favorably with the nominal a_T^2 of 33,534 $(ft/sec^2)^2$ and a_T of 5.7 g's.

Table 3-2. AC-8 Parking Orbit Parameters at T = 680.0 Seconds from 2-inch Motion Time
(MECO 1 + 101.54432 seconds)

SYSTEM	PERIGEE ALTITUDE (n.mi.)	APOGEE ALTITUDE (n.mi.)	PERIOD (min)	ORBIT INCLINATION (deg)	ENERGY (ft^2/sec^2)	ECCENTRICITY
NOMINAL	89.863	102.478	88.053	30.844	-0.65441599+09	0.00178
GUIDANCE (GET)	88.831	103.768	88.058	30.828	-0.65439215+09	0.00211
ACTUAL (BET)	89.013	104.290	88.071	30.826	-0.65432703+09	0.00216
GUID-NOM	-1.032	1.290	0.005	-0.036	23,840	0.00033
ACT.-NOM	-0.850	1.812	0.018	-0.018	88,960	0.00038

Table 3-3. Equation Branching and Programmed Events

EVENT	LOGICAL EQUATION TEST PASSED AND PARAMETERS	FLIGHT COMPUTER TIME (sec)	REMARKS
Initialize t_l, v_σ		0	Occurred 8.352 seconds prior to 2-in. motion
Flight Mode Accept Discrete (L9)		0.582	Issued at the end of initialization cycle
Enable BECO Acceleration Test*	$a_T^2 > E_2$ $E_2 = 10,000$ (ft/sec^2)^2	110.81307	$a_T^2 = 10,020$ (ft/sec^2)^2
BECO*	$a_T^2 > E_4$ $E_4 = 30,982.0$ (ft/sec^2)^2	149.67461	$a_T^2 = 32,024$ (ft/sec^2)^2
BECO Discrete (L3)		150.566	$a_T = 5.691$ g's
BECO Sensed*	$a_T^2 < E_5$ $E_5 = 2500.0$ (ft/sec^2)^2	152.83461	$a_T^2 = 1219.2$ (ft/sec^2)^2. Equations switch to Sustainer-Centaur first-burn mode
SECO Sensed*	$a_T^2 < E_7$ $E_7 = 550$ (ft/sec^2)^2	239.16692	$a_T^2 = 9.3$ (ft/sec^2)^2
SECO Backup Discrete (L6)		240.049	
First Burn MECO*	$\epsilon < E_6$ $E_6 = 0.1 \times 10^8$ (ft/sec)^2	581.78768	$\Delta t_{3O} = 1.09$ seconds. Switch to parking orbit equations
First Burn MECO Discrete (L16)		583.8074	Occurred 11 milliseconds early. (See Section 3.2)
Start Parking Orbit $\bar{f}^*$ Calculation*	$E_{12} < t_l - t_{MECO}$ $E_{12} = 5$ sec	589.39768	
VECO*	$J_{36} < t_l - t_{MECO}$ $J_{36} = 98.563845$ sec	682.97075	Start calculation of ϕ (parking orbit termination parameter)
VECO Discrete (L3)		683.852	
Second MES Sequence Initiated*	$\phi < o$	2017.0669	$\phi = -0.0006566$. Sigmators are rezeroed
Second MES Start Sequence Discrete (L6)		2018.019	
Second MES Sensed*	$a_T^2 > E_{13}$ $E_{13} = 550.0$ (ft/sec^2)^2	2087.4523	$a_T^2 = 1025$ (ft/sec^2)^2. Switch equations to Centaur second-burn mode
Second MECO*	$E_{15} < t_l - t_{MES}$ $E_{15} = 125.0$ sec	2213.3322	Second MECO was issued on a time backup test
Second MECO Discrete (L16)		2214.232	
Calculate Reorient Vector ($\bar{i}^* = -\bar{v}_M$)*	$E_{16} < t_l - t_{MECO}$ $E_{16} = 60.0$ sec	2273.8769	
Calibrate Telemetry on Discrete (L8)	$E_{18} < t_l - t_{MECO}$ $E_{18} = 88.7$ sec	2303.147	
Calibrate Telemetry Off Discrete (L10)	$E_{19} < t_l - t_{L8}$ $E_{19} = 3.48$ sec	2307.379	

* Indicates equation branching

SECO. SECO was issued by the Centaur autopilot at 237.769 seconds (computer time) based upon fuel depletion. SECO is "A" timer zero time. First MECO and VECO enable and backups are issued with respect to this event. The sustainer engines began shutting down at 237.812 seconds. The guidance equations issued a backup SECO discrete (L6) at 240.049 seconds when $a_T^2 < 550.0$ $(ft/sec^2)^2$.

First MECO. First MECO was enabled by the autopilot 325.5 seconds after SECO or at 563.269 seconds of computer time. MECO was issued by the guidance equations on an energy-to-be-gained criteria at 583.8074 seconds. This occurred approximately 5.46 seconds prior to autopilot MECO time backup.

The time to cutoff, Δt_{CO}, was telemetered as 1.09 seconds. Energy-to-be-gained to cutoff was checked by three different methods. The three results agreed within 30 $(ft/sec)^2$, with an average error of 37,000 $(ft/sec)^2$. Since $\dot{\epsilon}$ was 0.336×10^7 ft^2/sec^3, the cutoff extrapolation error was determined to be 11 milliseconds early. This corresponds to a velocity error of 0.7 ft/sec. During first burn, the PU valve was not nulled prior to cutoff, as it would have been prior to second burn cutoff. However, an analysis of PU valve motion immediately preceding first MECO indicated that no cutoff error was introduced due to PU effects. A study of the effect of accelerometer limit cycles on cutoff (Analysis of Guidance MECO Error Sources for Atlas/Centaur Missions, GDC-BTD66-041, 18 April 1966) indicates that cutoff could be in error by $\pm$ 30 milliseconds (3σ value) due to the quantitization effect. The actual cutoff error was well within this.

Analysis of accelerometer Δv pulse data immediately following MECO indicated that the shutdown impulse was 2800 $\pm$ 110 lb-sec. This differs by 100 lb-sec from the targeted value of 2700 lb-sec, corresponding to a velocity error of 0.23 ft/sec.

VECO. VECO was enabled by the autopilot at first MECO time backup (589.27 seconds). VECO was commanded by the guidance L3 discrete at 683.852 seconds (computer time). This occurred approximately 5.32 seconds prior to autopilot VECO backup.

Second MES Sequence. Guidance "MES sequence initiated" occurred at 2018.019 seconds (computer time). The sigmators were rezeroed at this time, and the guidance equations again start to process accelerometer output. This occurred approximately 19.9 seconds prior to the beginning of the 100-pound thrust during the vernier engines one-half on phase.

Second MECO. Since the desired energy was not achieved, the guidance equations exercised the time backup branch to issue the L16 (second MECO) discrete. This occurred approximately 23 seconds after the nominal preflight MECO time. Since the reorient vector calculation and the issuance of the L8 and L10 discretes are dependent on the time from second MECO, they also occurred approximately 23 seconds late, although they occurred at the proper time with respect to actual second MECO.

3.3 GUIDANCE TRAJECTORY DATA. For reference purposes, trajectory parameters and gyro torquing rates computed during the flight by the airborne computer are shown in Figures 3-2 through 3-9. The nominal values are not shown, since the actual trajectory compares closely with the nominal until second burn.

The plots of $\bar{r}_T$ and $\bar{v}_T$ in Figures 3-6 and 3-7 are sigmator values corrected for accelerometer scale factor (D_1, D_2, D_3). The plot of required velocity in t, n, r coordinates in Figure 3-8 does not include the radial component (v_{rr}), as this is not calculated during the Centaur first burn.

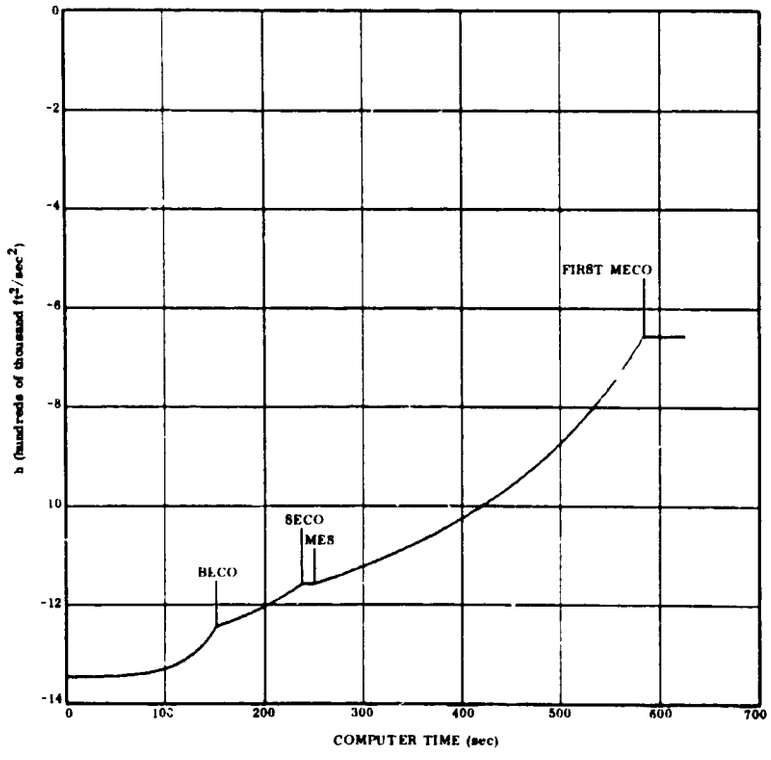

Figure 3-2. Orbital Energy per Unit Mass, h

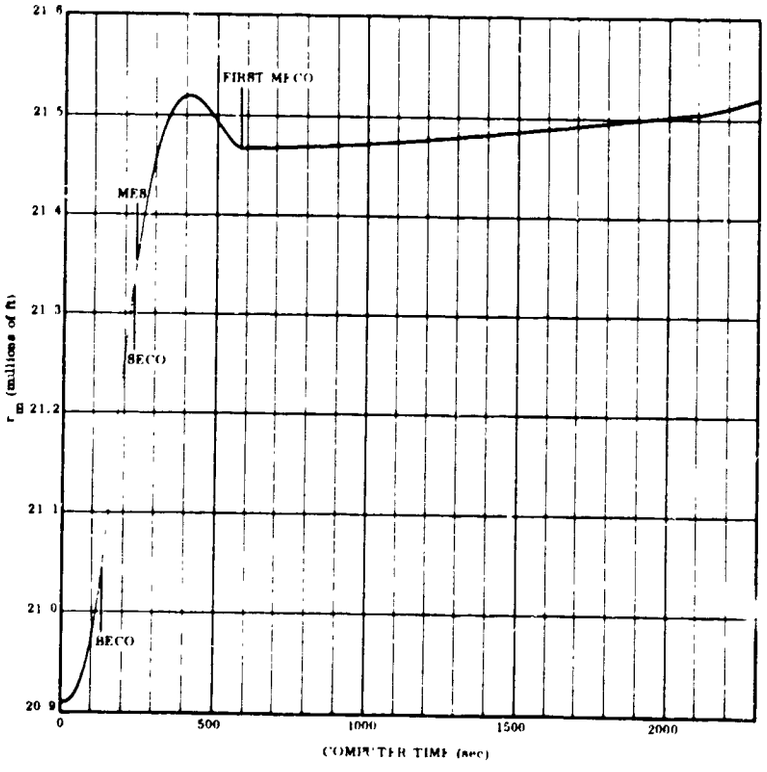

Figure 3-3. Inertial Position Magnitude, r_m

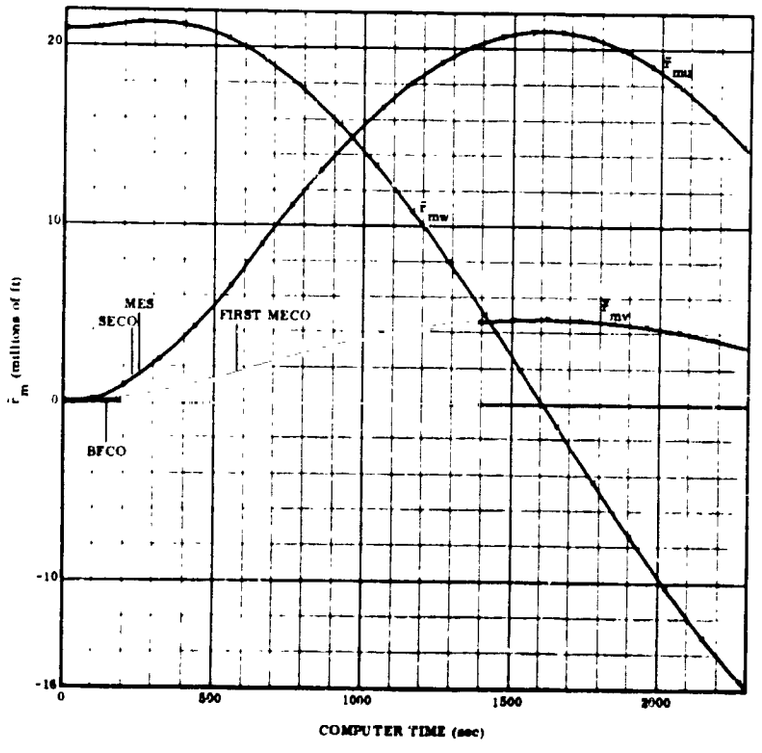

Figure 3-4. Vehicle Inertial Position, $\bar{r}_m$

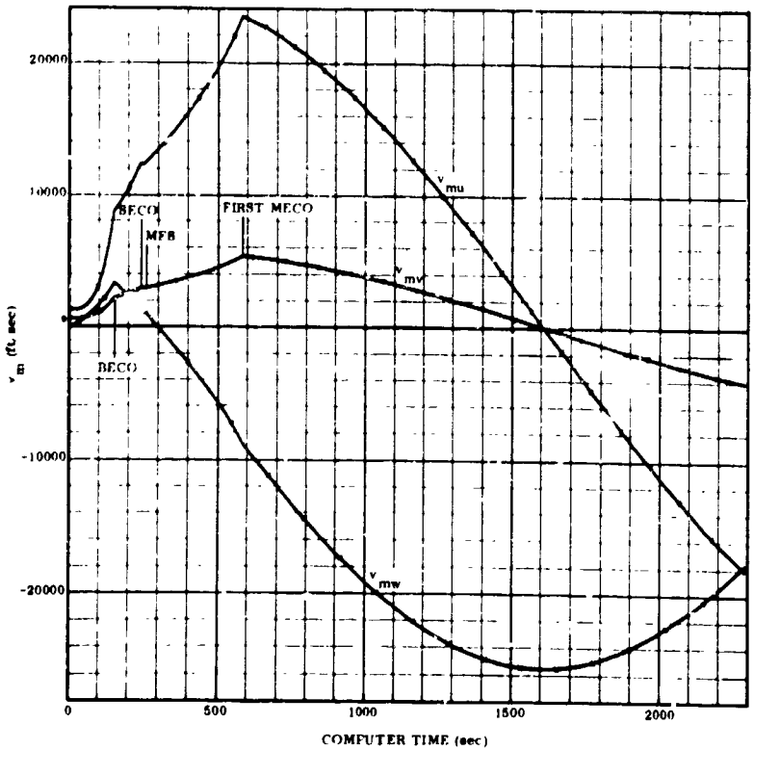

Figure 3-5. Vehicle Inertial Velocity, $\bar{v}_m$

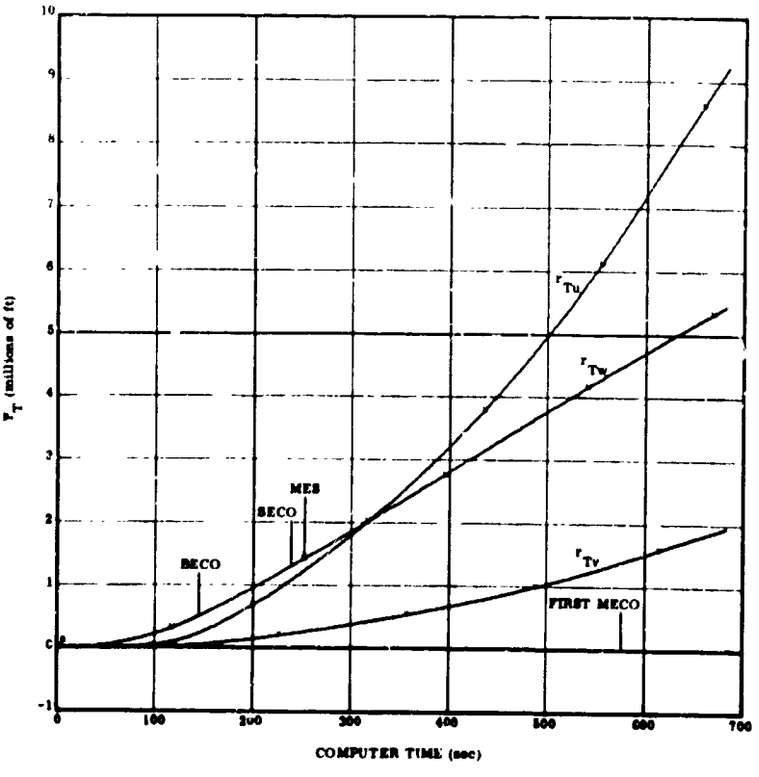

Figure 3-6. Thrust Position, $\bar{r}_T$

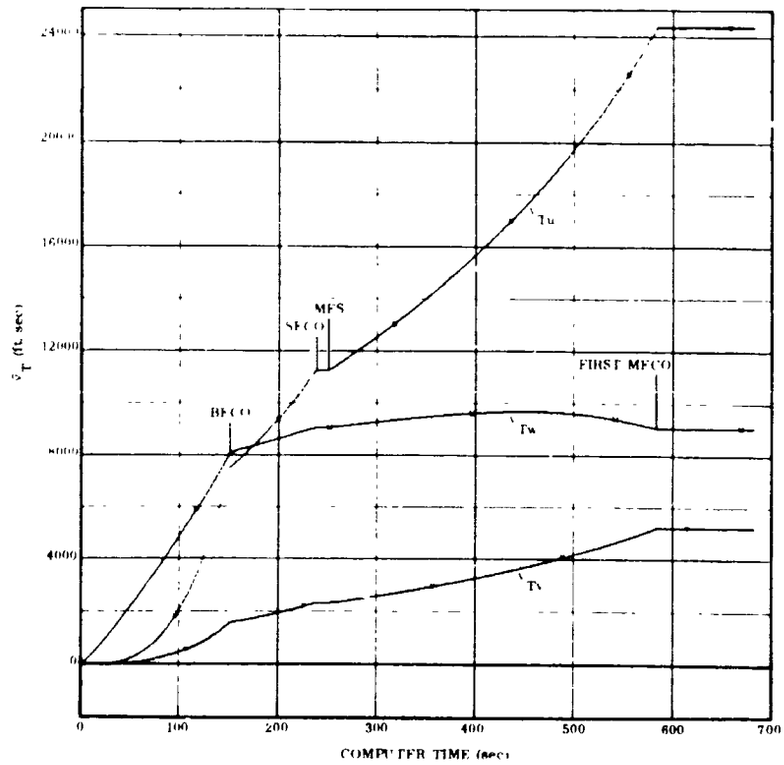

Figure 3-7. Thrust Velocity, $\bar{v}_T$

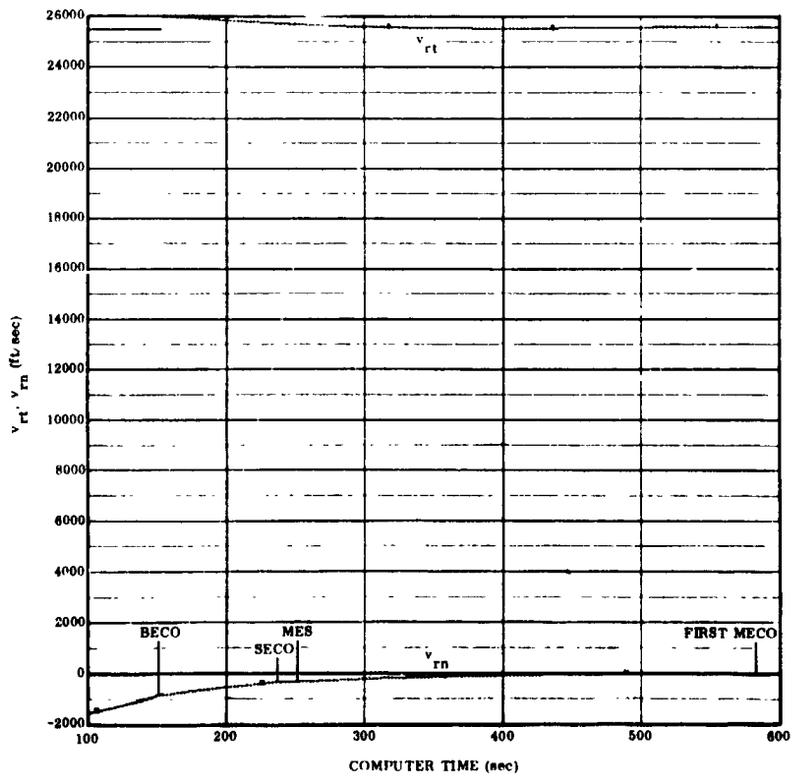

Figure 3-8. Required Velocity in Rotating t, n, r Coordinates

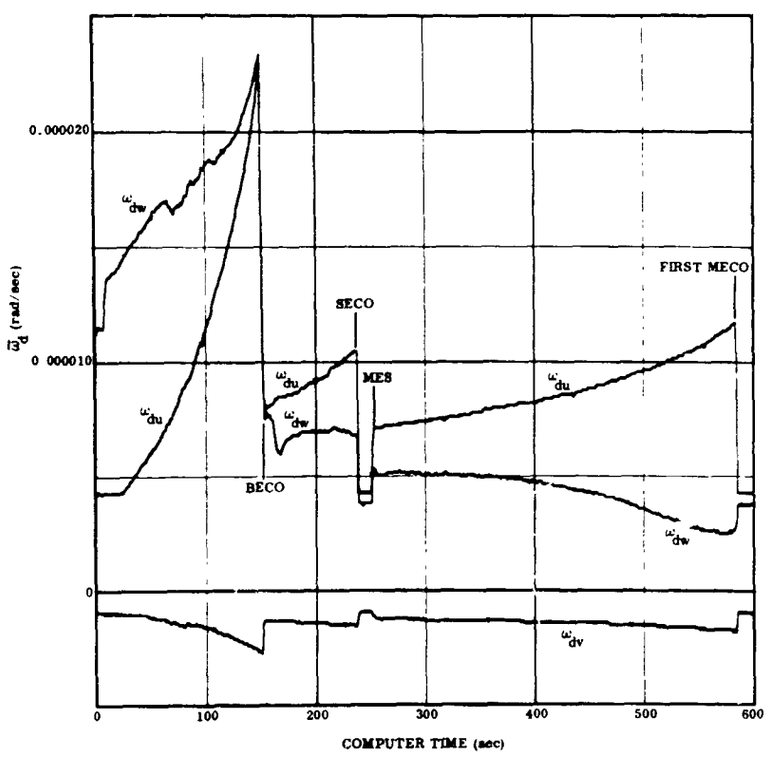

Figure 3-9. Gyro Torquing Rate, $\bar{\omega}_d$

SECTION 4

GUIDANCE STEERING ANALYSIS

Guidance-controlled vehicle attitude steering is used to correct trajectory dispersions and thereby achieve the proper velocity and position vectors at first and second MECO. The steering is also designed to make the launch vehicle fly an optimum trajectory to maximize payload.

There is no guidance steering during booster stage. Guidance steering is enabled by the autopilot during the following intervals:

a. BECO + 8 seconds to SECO

b. First MES + 4 seconds to second MES

c. Second MES + 4 seconds to second MECO

d. Continuously from second MES + 181 seconds

4.1 ATTITUDE STEERING. Guidance steering is accomplished by calculating a desired thrust pointing direction, $\bar{f}$, which is a modified velocity-to-be-gained vector. An integral control term, $\overline{\Delta f}$, is added to $\bar{f}$ giving the actual output steering vector $\bar{f}^*$. The integral control term, $\overline{\Delta f}$, compensates for thrust misalignments, errors in the control loop, and control system lags. When the vehicle axis is aligned to $\bar{f}^*$, the thrust vector should be aligned to $\bar{f}$.

The output steering vector, $\bar{f}^*$, is converted to an analog signal and input to the resolver chain. Error signals from the resolver chain output amplifiers generate turning rates in the autopilot to cause the vehicle roll axis to be aligned with $\bar{f}^*$.

The modified velocity-to-be-gained vector, $\bar{f}$, computed during the flight, is shown in Figure 4-1. The output steering vector, $\bar{f}^*$, is shown in Figure 4-2. Until second MES, both sets of curves closely matched the expected nominal values. Therefore the nominal is not shown.

Actual vs Desired Thrust Direction. If the steering loop functions properly, the vehicle thrust acceleration vector, $\bar{a}_T$, will line up with $\bar{f}$. The angle, θ, between $\bar{a}_T$ and $\bar{f}$ was therefore computed and is shown in Figures 4-3 through 4-6. Both the nominal and flight values are shown. The angular components are defined such that a positive rotation of $\bar{a}_T$ through the angles θ_u, θ_v, and θ_w would make it colinear with $\bar{f}$. It is apparent from the curves that the steering loop kept the vehicle thrust vector closely aligned with the velocity-to-be-gained vector.

Integral Control Term. The nominal and flight values of the integral control term, $\overline{\Delta f}$, is shown plotted in Figure 4-7. No significant difference occurred.

Since the integral control term represents the angular difference between $\bar{f}$ and $\bar{f}^*$, the angle between them, Ψ, was computed to better describe this correction. The components and magnitude of Ψ are shown plotted in Figures 4-8 through 4-11. The components are defined such that a positive rotation of $\bar{f}^*$, about the u, v, and w axis makes $\bar{f}^*$ colinear with $\bar{f}$.

The nominal values of Ψ_u and Ψ_v are primarily corrections for computation lags and thrust misalignments. The flight values of Ψ_v and Ψ_w show shifts from nominal during Centaur stage of 0.3 and 0.4 degrees respectively. These might be corrections for resolver chain errors or thrust misalignments. These errors are well within the resolver chain accuracy specification of 2 degrees.

4.2 ALTITUDE CONTROL. One of the functions of the steering equations during first burn is to control the parking orbit insertion altitude. Steering is based upon adjusting the pitch shaping function, G_r, according to the difference between r_{nom} and r_m where

$$r_{nom} = K_{14} + K_{15}\, t_b + K_{16}\, t_b^2 + K_{17}\, t_b^3 .$$

The difference between the nominal value of r_m derived from a preflight simulation and the flight value of r_m is shown in Figure 4-12. It is apparent from the curve that Δr_m was kept to within approximately 6000 feet of the desired nominal. This is well within the software specification of 3.5 n.mi. The drop after MES appears to be due to a low radial component of velocity at SECO. The difference between the flight and nominal value of radial velocity, v_{mr}, is shown in Figure 4-13.

4.3 YAW STEERING. Yaw steering is used to achieve the proper orbital plane. A comparison of the nominal and flight yaw error signal, $\dot{\epsilon}_y$, is shown in Figure 4-14. A small shift of $\dot{\epsilon}_y$ from nominal appeared at the beginning of steering. It is apparent that the guidance equations successfully removed the yaw error.

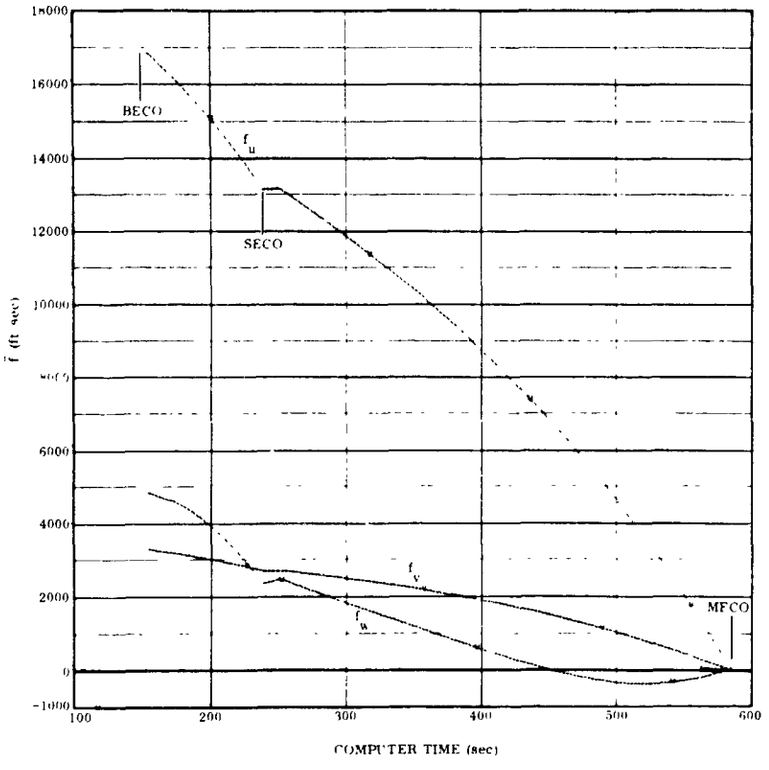

Figure 4-1. Desired Thrust Attitude, $\bar{f}$

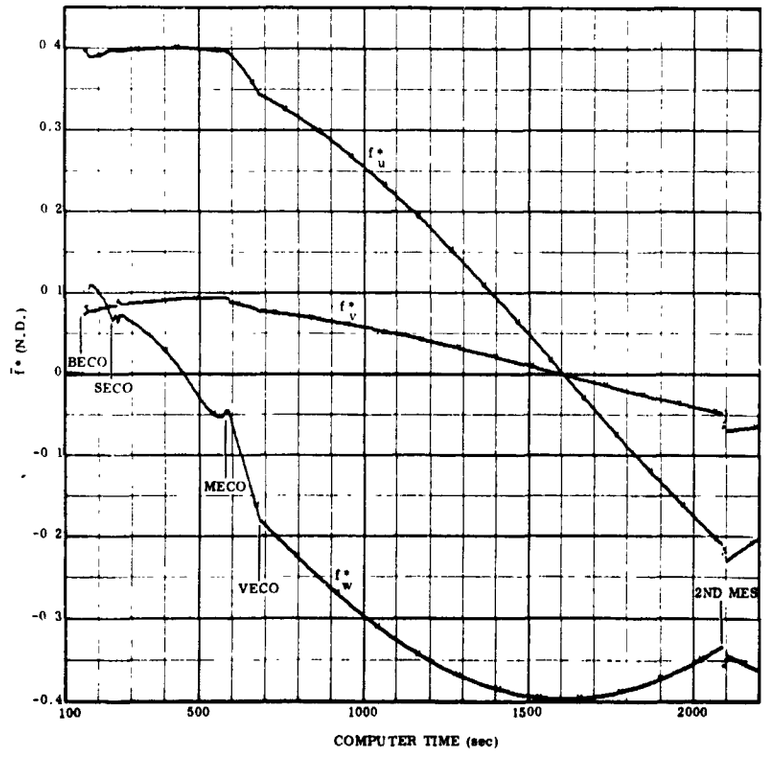

Figure 4-2. Steering Vector, $\bar{f}^*$

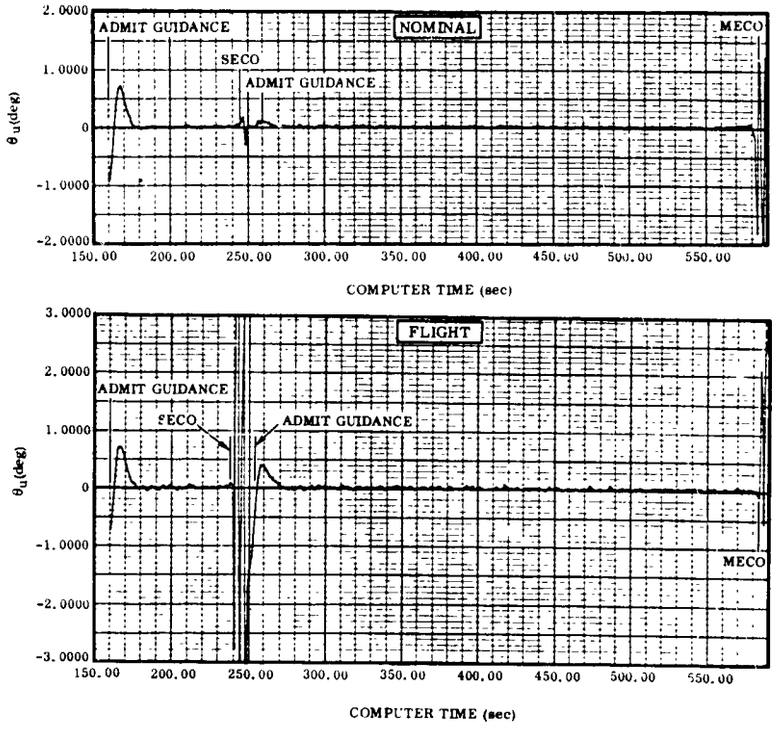

Figure 4-3. θ_u

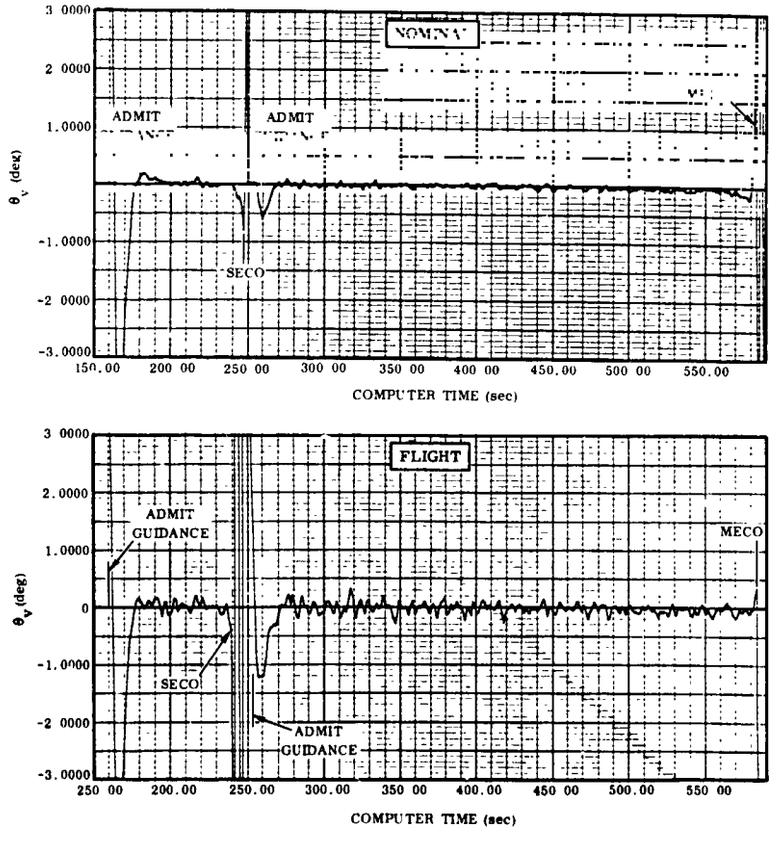

Figure 4-4. θ_v

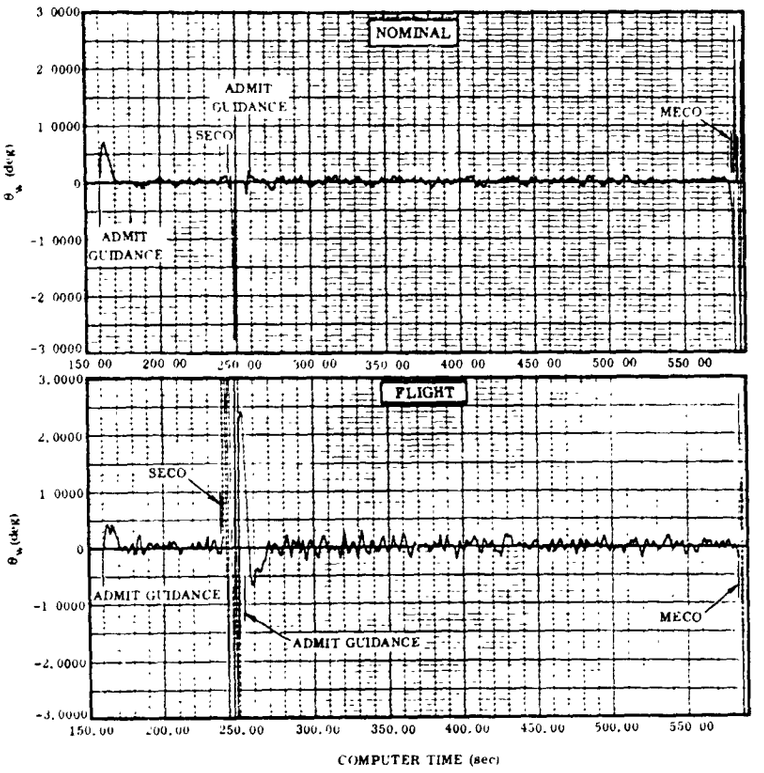

Figure 4-5. θ_W

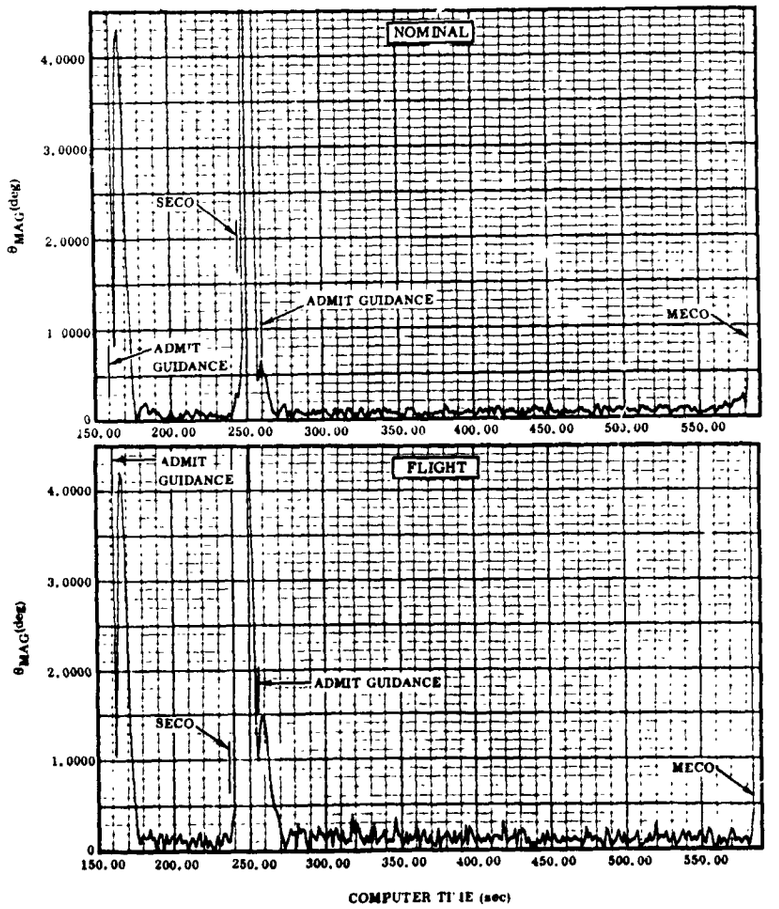

Figure 4-6. θ_{MAG}

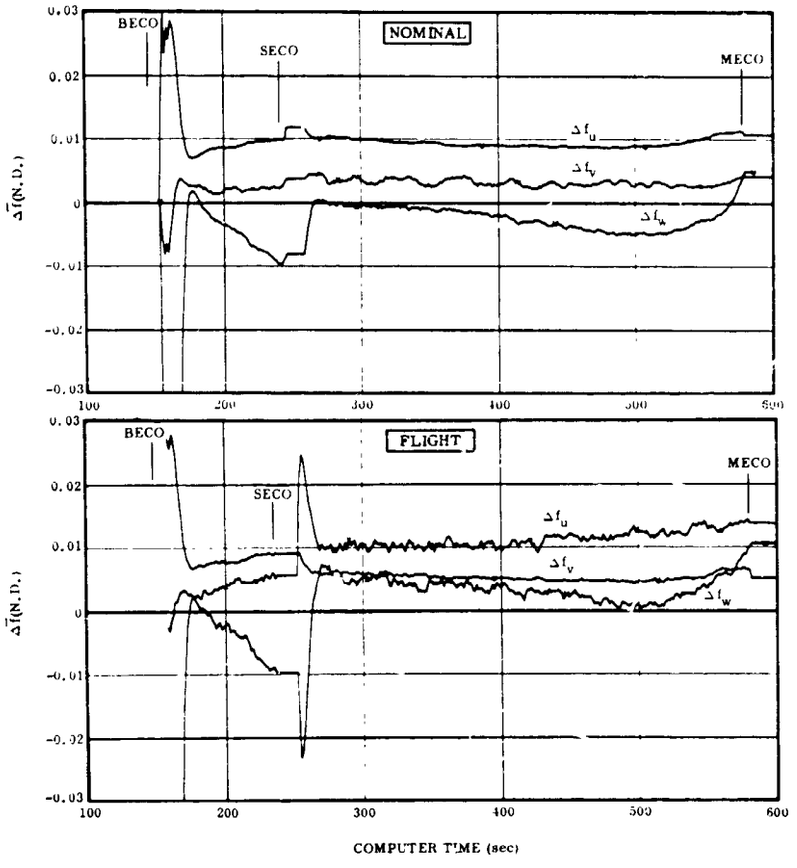

Figure 4-7. Integral Control Term, $\overline{\Delta f}$

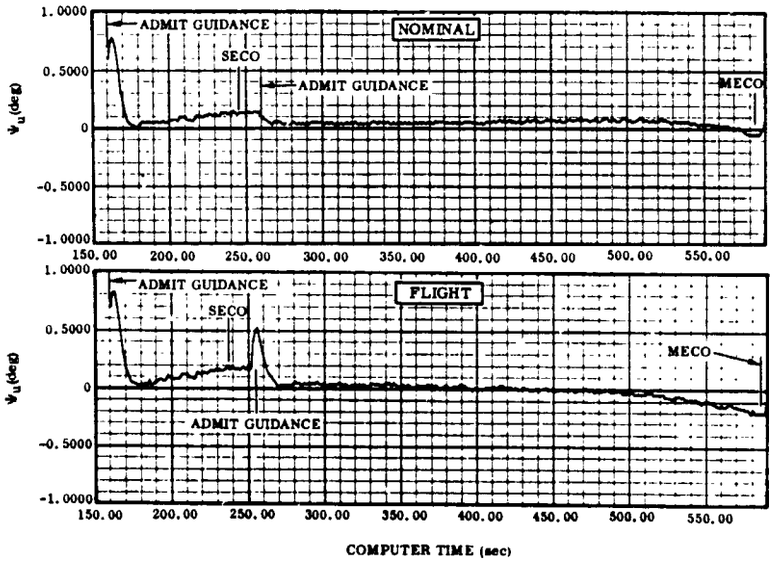

Figure 4-8. Ψ_u

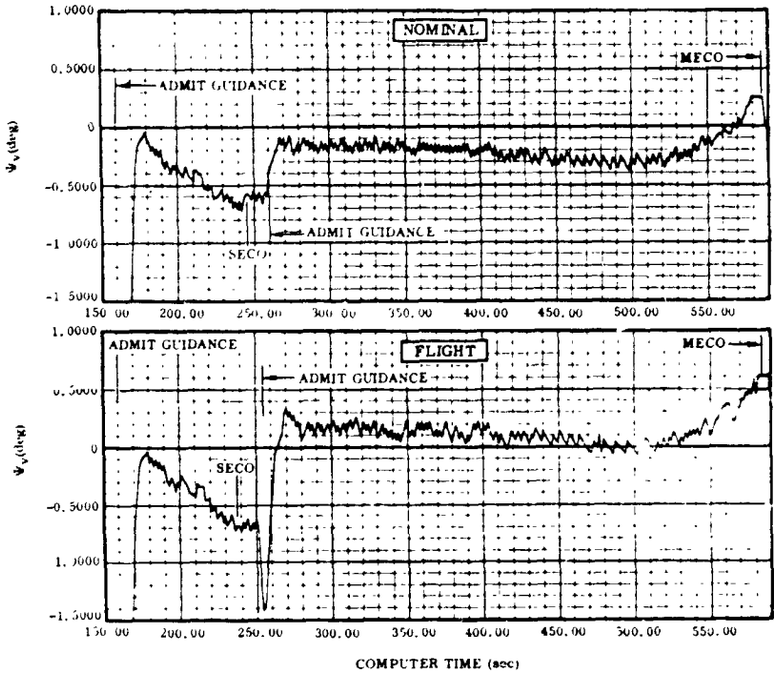

Figure 4-9. Ψ_V

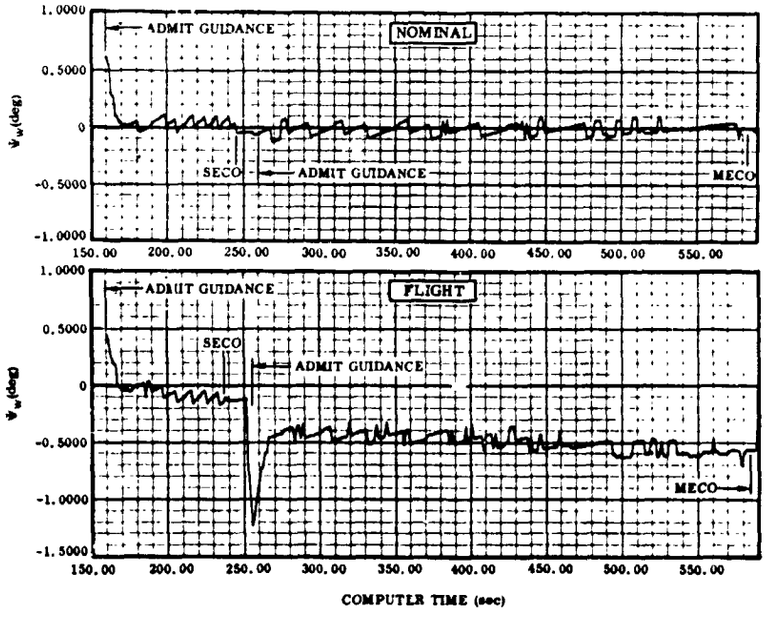

Figure 4-10. Ψ_W

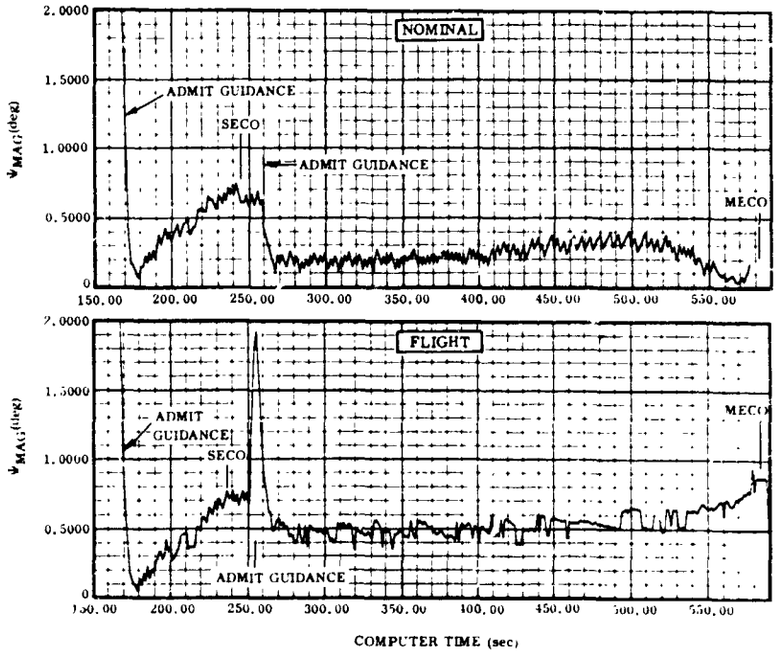

Figure 4-11. Ψ_{MAG}

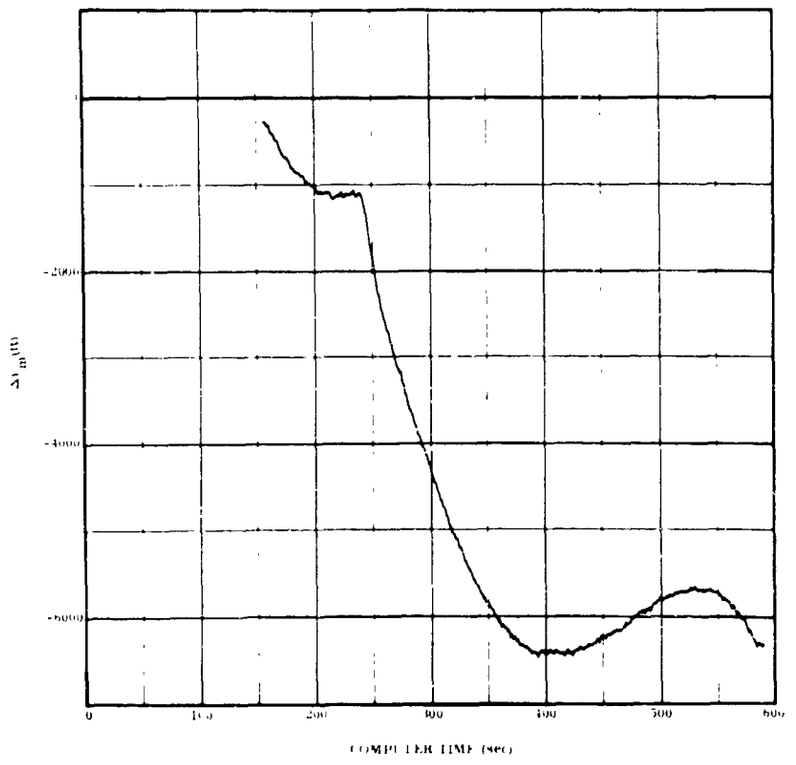

Figure 4-12. Δr_m

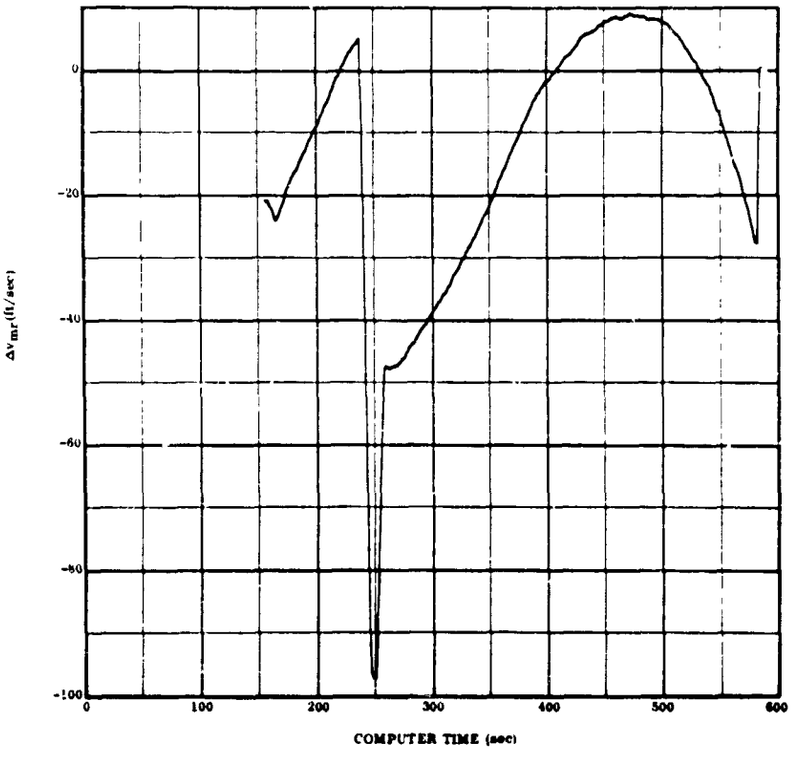

Figure 4-13. Δv_{mr}

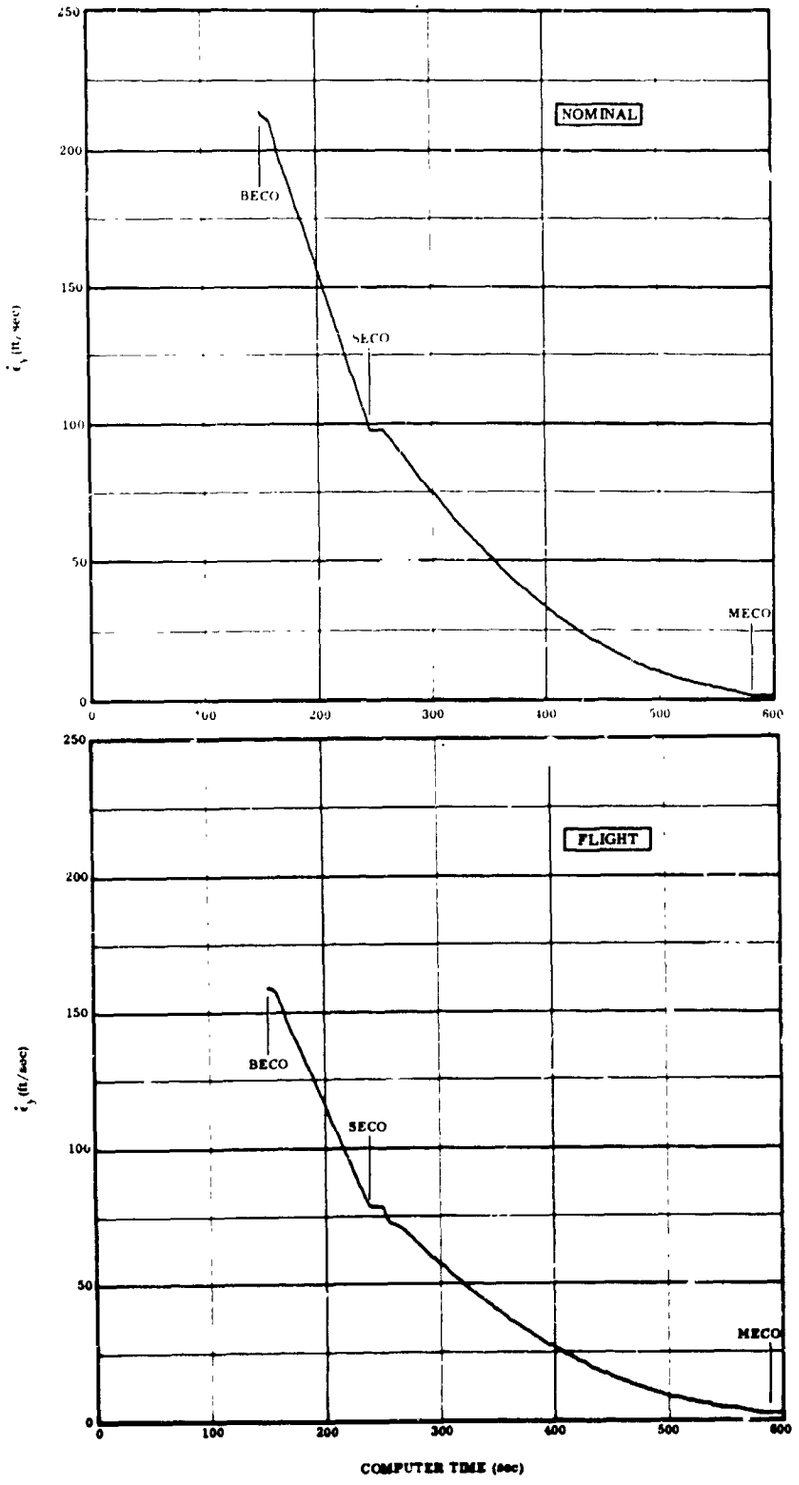

Figure 4-14. Yaw Error Signal, $\dot{\epsilon}_y$

SECTION 5

VELOCITY COMPARISON

5.1 TRACKING DATA FOR AC-8. Powered-flight thrust velocity profiles based on ground tracking data were compared with telemetered guidance system values in order to determine guidance system errors. The trajectory data available for the AC-8 flight consisted of Azusa Mk II and ETR-produced Best Estimated Trajectory (BET) tracking data. The coverage intervals for the uprange tracker sites used in acquiring the raw BET data are shown in Figure 5-1.

The Azusa data were supplied from 16.96 to 202.66 seconds and 203.26 to 439.21 seconds after liftoff. The data were supplied every 0.05 second in pad-centered, earth-rotating x, y, z coordinates. These data were not used in the guidance evaluation since the estimates of the Azusa velocity errors were too large for guidance error analysis.

The uprange BET data covered the period from 22.21 to 715.21 seconds after liftoff. The data were supplied every 0.5 second in earth-centered, inertial u, v, w coordinates with the covariance matrix on the tape. After 600 seconds, the data became meaningless from the standpoint of guidance evaluation due to the very large uncertainties in the data. The range estimates of total errors in the uprange BET are presented in Figures 5-2, 5-3 and 5-4.

The downrange BET was not used for guidance evaluation since the estimates of velocity errors were an order of magnitude larger than the guidance system errors.

5.2 HANDOVER. For AC-8, handover of data to Bermuda occurred between 420 and 440 seconds after liftoff. The transition was much smoother than for previous flights.

5.3 VELOCITY COMPARISON. A new IBM 7094 computer program has been developed to perform the velocity comparison for AC-8. Unlike the previous program, the current program calculates a true (or non-zero-set) thrust velocity error by using guidance vehicle position ($\bar{r}_{m_i}$) to calculate the velocity component due to gravity prior to acquisition of tracking data.

The true thrust velocity errors (guidance $\bar{v}_T$ - tracker $\bar{v}_T$) are shown in Figures 5-5, 5-6 and 5-7, in the u, v, and w directions; these plots start at the beginning of tracking data and end at 600 seconds after liftoff because of very large uncertainties in the data past that point. (The differences include corrections to the guidance data for accelerometer bias, scale factor, misalignments, and platform azimuth orientation, d_{19}.) The time reference for the plots is 2-inch motion.

The velocity errors for AC-8 were smaller than the values observed on the previous flight (AC-6). The values at MECO are approximately -0.5 ft/sec, -3.3 ft/sec, and -4.2 ft/sec for the u, v, and w components respectively. At the corresponding time for the AC-6 flight, the errors were approximately 6.5 ft/sec, -1.5 ft/sec, and 12 ft/sec. It should be emphasized that the velocity errors include both tracker and guidance system errors. It is assumed that the major contribution of error was the guidance system since the tracker estimates of error were small.

The guidance $\bar{v}_m$ telemetered data were adjusted to real world values and compared with the BET $\bar{v}_m$. The resulting error curves were essentially the same as Figures 5-5, 5-6, and 5-7. The corresponding velocity errors at MECO were approximately -0.4 ft/sec, -3.1 ft/sec, and -4.7 ft/sec.

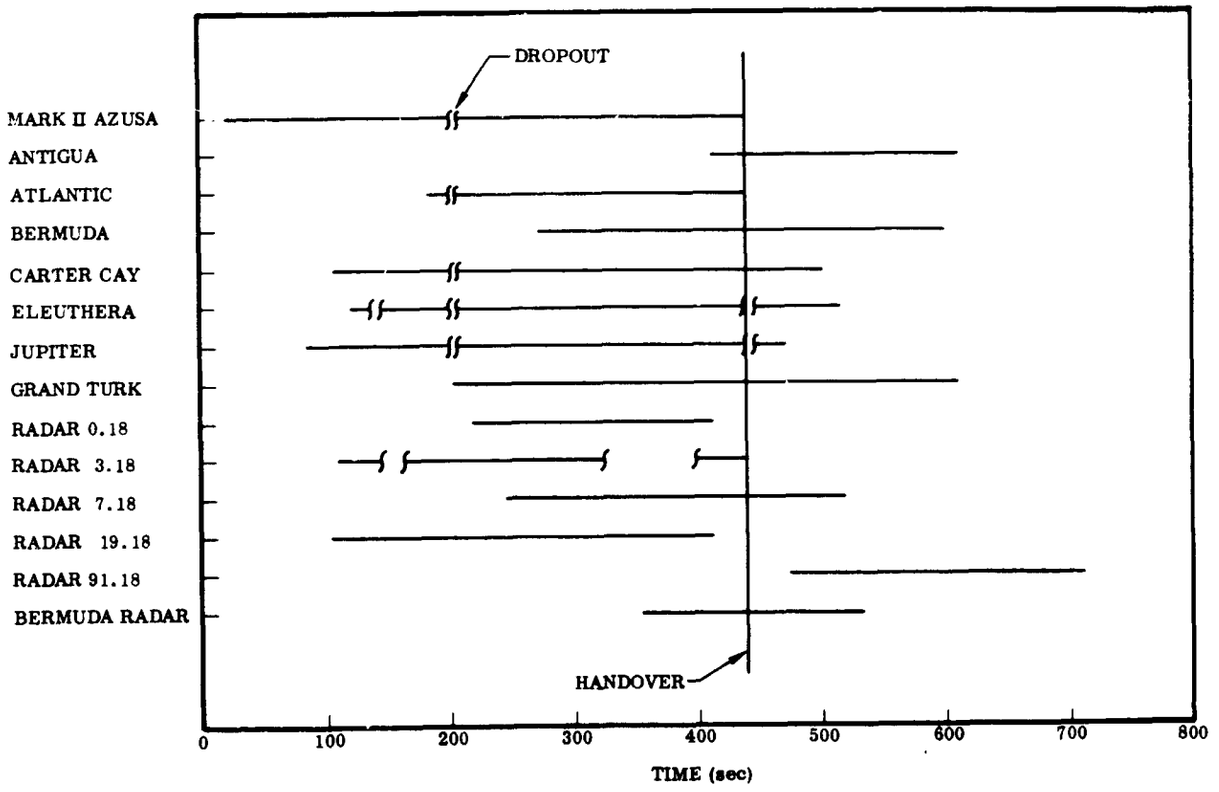

Figure 5-1. Tracking Data Used in Uprange AC-8 BET

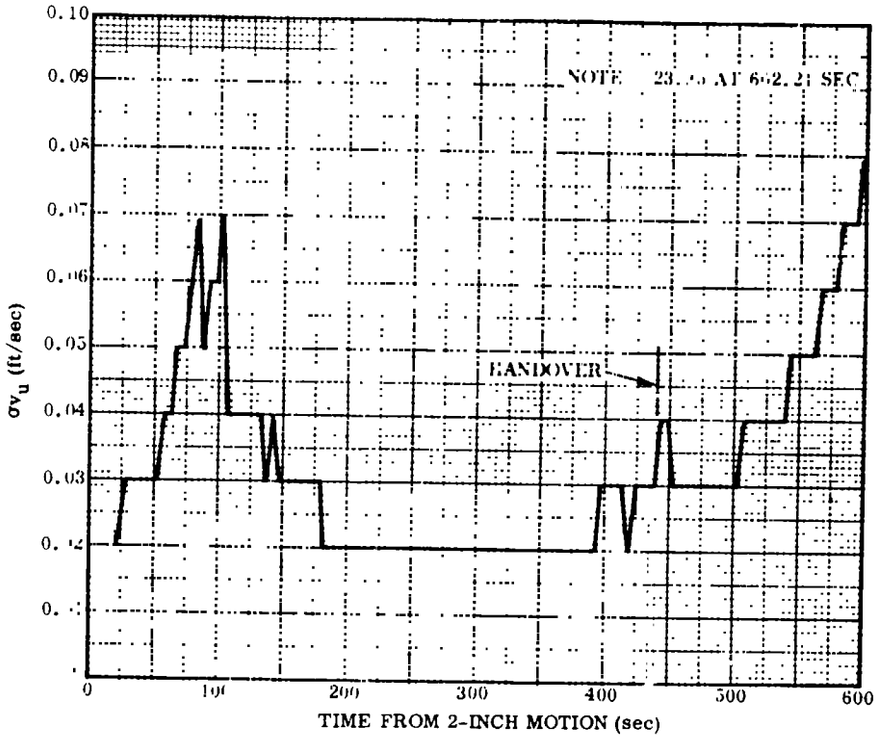

Figure 5-2. Range Estimate of Error in u Velocity

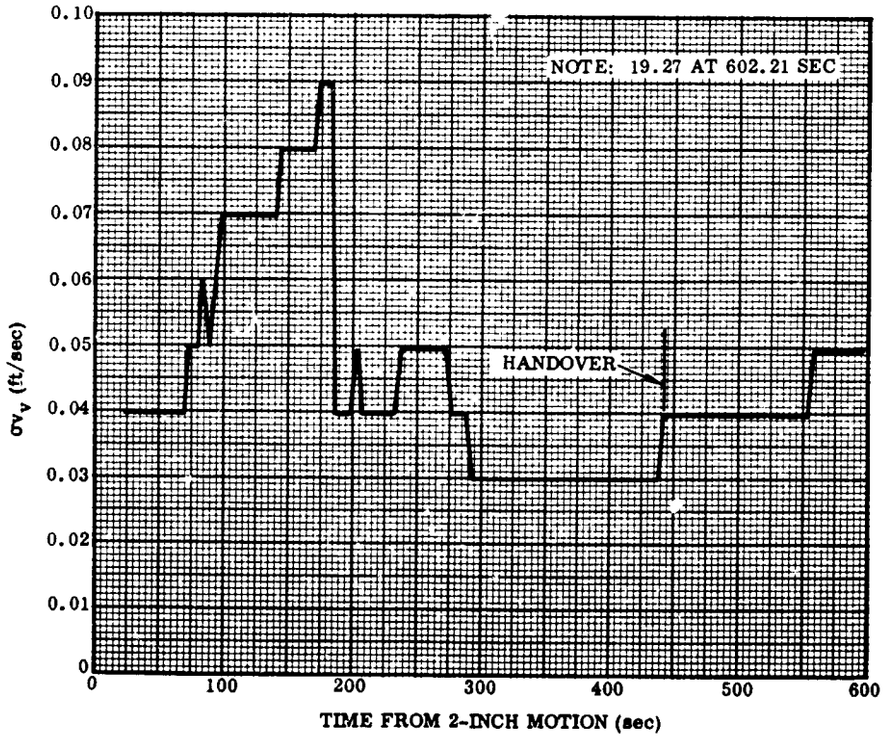

Figure 5-3. Range Estimate of Error in v Velocity

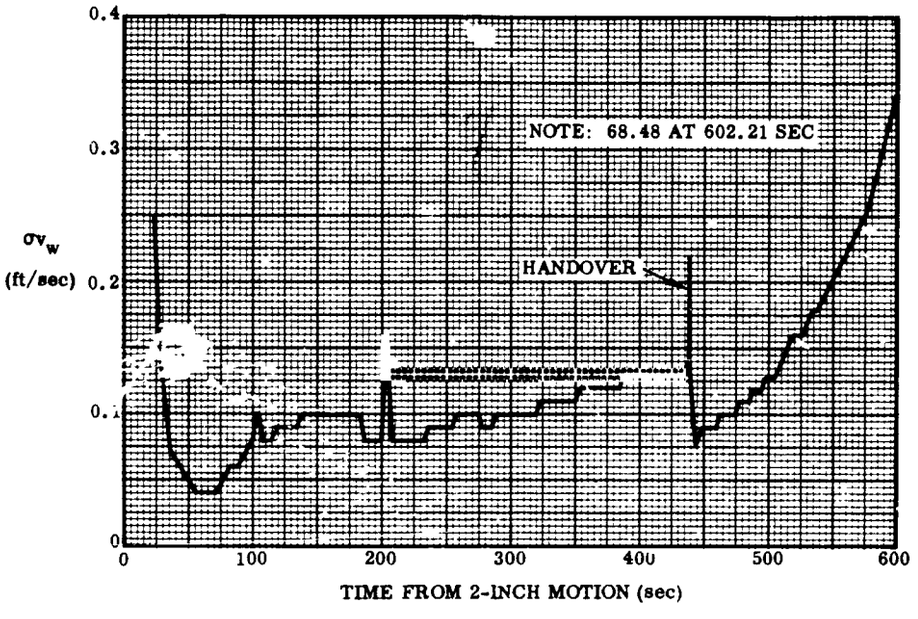

Figure 5-4. Range Estimate of Error in w Velocity

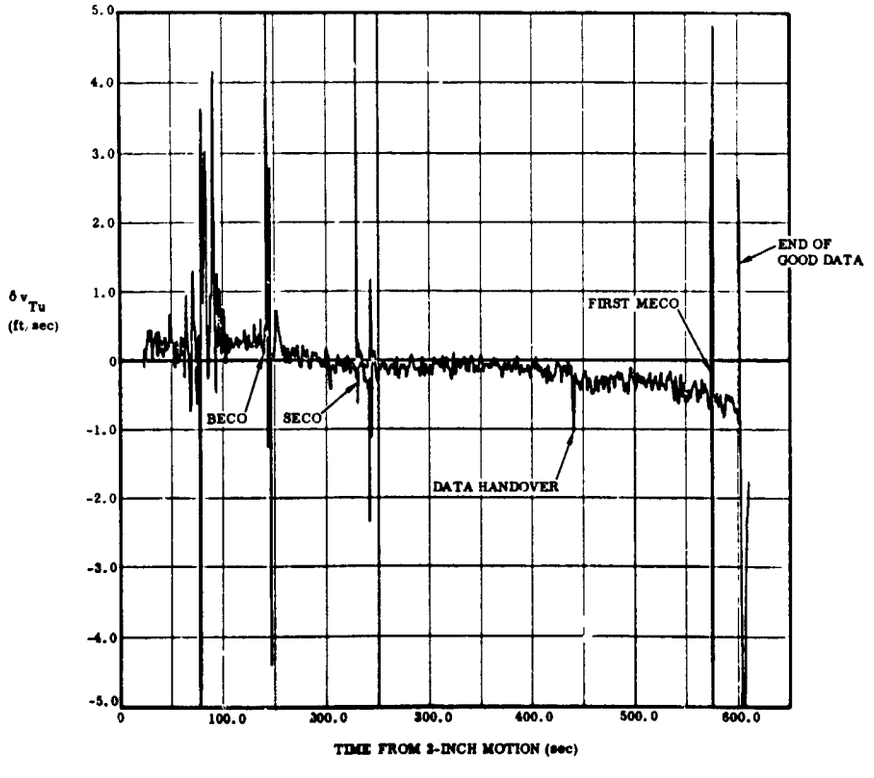

Figure 5-5. δV_{Tu} versus Time

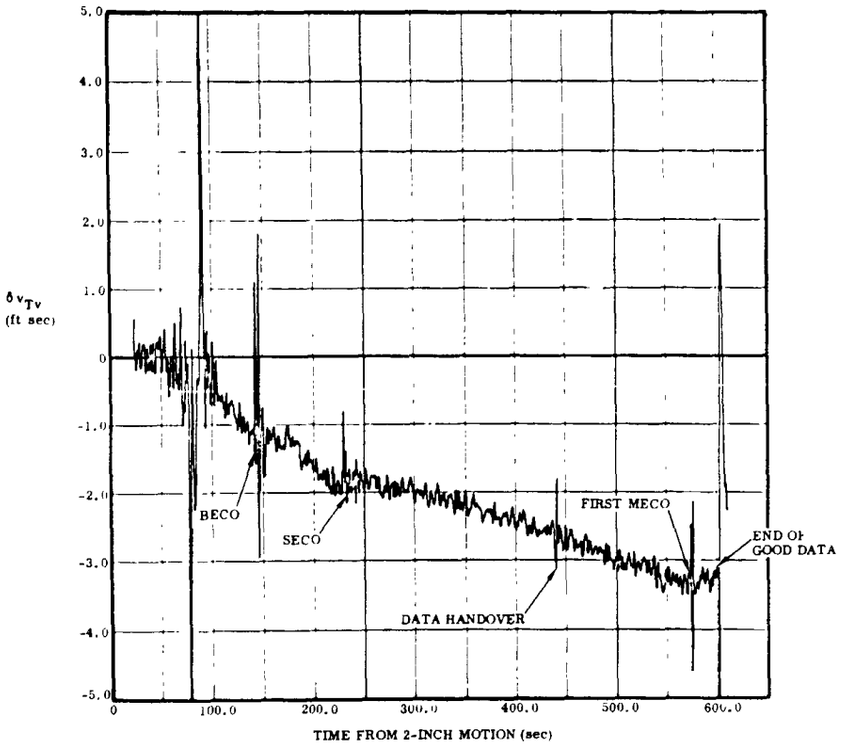

Figure 5-6. δV_{Tv} versus Time

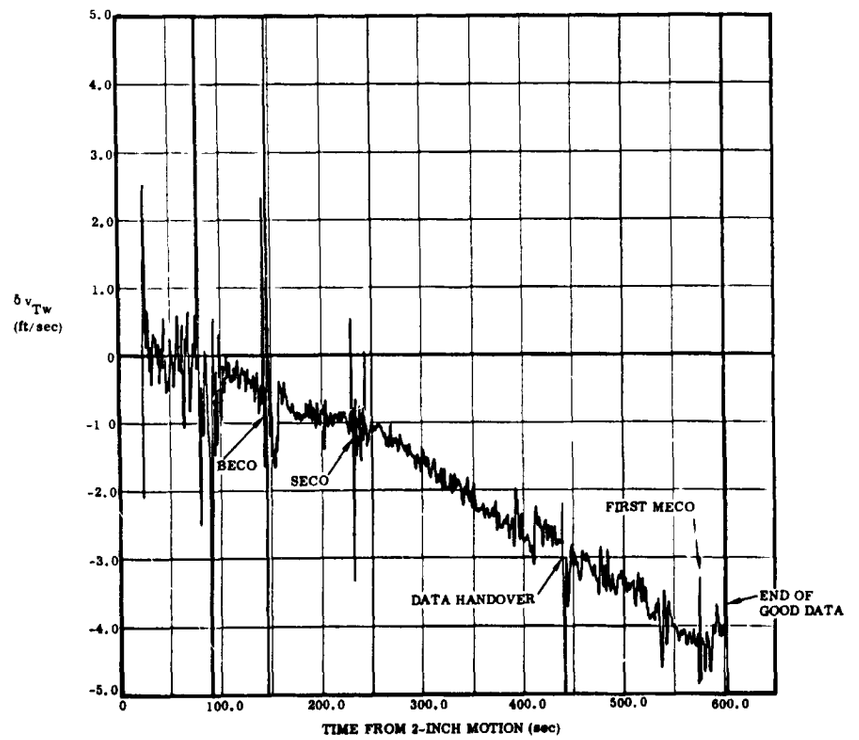

Figure 5-7. δV_{Tw} versus Time

SECTION 6

ERROR SEPARATION

The velocity-error histories during powered flight, shown in Figures 5-5 through 5-7, were analyzed to determine the individual sources of error. The error separation results, based upon the ETR BET, are presented in this section.

6.1 ERROR MODEL. The guidance system error model assumed in the analysis is shown in Table 6-1. The first 18 errors correspond to shifts or errors in the calibrated d values.

No significant second-degree errors showed up in the analysis and were therefore not considered in the error separation.

The error model is idealized in that it assumes that the guidance errors remain constant throughout the flight. Most of the errors are expected to shift somewhat, particularly since they are affected by a changing thermal and vibration environment during flight.

6.2 ACCELEROMETER BIAS. The first errors determined were accelerometer biases. They were calculated from the 6-pound thrust "coast period" that began 100 seconds after first MECO. A recently developed computer program, the Freefall Acceleration Bias program (FAB) was used to calculate the expected thrust velocities along each inertial axis during the coast period. These velocities were then subtracted from the telemetered thrust velocities. The velocity differences were fitted by a least squares technique to both first- and second-degree curves, $f(x) = a_0 + a_1 x$ and $f(x) = a_0 + a_1 x + a_2 x^2$. The slope of the curve, a_1, is the bias error. The value of a_1 for both solutions agreed. The nominal thrust value for each of the four S engines was 3.1 pounds. It was expected that two of them would operate simultaneously for a total thrust of 6.2 pounds. The solution appeared to indicate that the actual average thrust was 10 percent low, i.e., 5.6 pounds, and that there was no thrust between 1,500 and 1,580 seconds. The bias errors during the no-thrust time period agreed with the values obtained earlier and are shown below; it is apparent that these errors are well within specification values.

DIRECTION	ERROR SYMBOL	BIAS ERROR (ft/sec^2)	BIAS ERROR (μg)	55-04040F SPEC (μg)
u	ϵ_7	+0.0007	22	300
v	ϵ_8	+0.0007	22	480
w	ϵ_9	-0.0019	-59	480

Table 6-1. Error Model

SYMBOL	ERROR
ϵ_1	u accelerometer scale factor
ϵ_2	v accelerometer scale factor
ϵ_3	w accelerometer scale factor
ϵ_4	Misalignment of v accelerometer with respect to u accelerometer
ϵ_5	Misalignment of w accelerometer with respect to u accelerometer
ϵ_6	Misalignment of w accelerometer with respect to v accelerometer
ϵ_7	u accelerometer bias error
ϵ_8	v accelerometer bias error
ϵ_9	w accelerometer bias error
ϵ_{10}	u gyro fixed torque drift
ϵ_{11}	u gyro input axis mass unbalance drift
ϵ_{12}	u gyro spin axis mass unbalance drift
ϵ_{13}	v gyro fixed torque drift
ϵ_{14}	v gyro input axis mass unbalance drift
ϵ_{15}	v gyro spin axis mass unbalance drift
ϵ_{16}	w gyro fixed torque drift
ϵ_{17}	w gyro input axis mass unbalance drift
ϵ_{18}	w gyro spin axis mass unbalance drift
ϵ_{31}	Initial platform misalignment about u axis
ϵ_{32}	Initial platform misalignment about v axis
ϵ_{33}	Initial platform misalignment about w axis

6.3 ERROR SEPARATION RESULTS. Assuming the bias errors indicated in the previous section, the velocity errors were analyzed to determine the remaining individual guidance error sources.

The gimbal motor demodulator outputs telemetered during flight indicated that, beginning with the booster pitch program, the platform had an average tilt error of approximately 7 arc seconds. The direction of this tilt caused the u and w accelerometers to sense some accelerations in the -w and u directions respectively. This error can be approximated by assuming ϵ_{32} = 7 arc seconds.

With this error removed, the remaining velocity residuals were studied to determine their probable source. Although these errors are smaller than those found in any previous flight and that guidance and tracker noise represents a significant portion of the velocity residuals, the additional errors shown in Table 6-2 appeared to be likely. These errors appear to be well within the specification limits.

The guidance and tracking velocity differences are so small that it is not possible to prove that any particular combination of errors that match the velocity residual curves are the actual errors that existed. The Table 6-2 errors are reasonable considering the shifts measured during preflight calibration of the guidance system. Refer to Figures 6-1, 6-2, and 6-3 for plots of the individual errors and Figures 10-1 through 10-6 for plots of the preflight calibration history.

Table 6-2. Residual Velocity Errors

ERROR	VALUE	55-04040F MAX SPEC
u-Accelerometer Scale Factor	ϵ_1 = -0.004%	0.021%
v-Accelerometer Misalignment with Respect to the u Axis	ϵ_4 = -35 arc sec	93 arc sec
Platform Misalignment about the v Axis	ϵ_{32} = 7 arc sec	15 arc sec (inflight static)
v-Gyro MUIA Drift	ϵ_{14} = 0.10 deg/hr/g	0.36 deg/hr/g

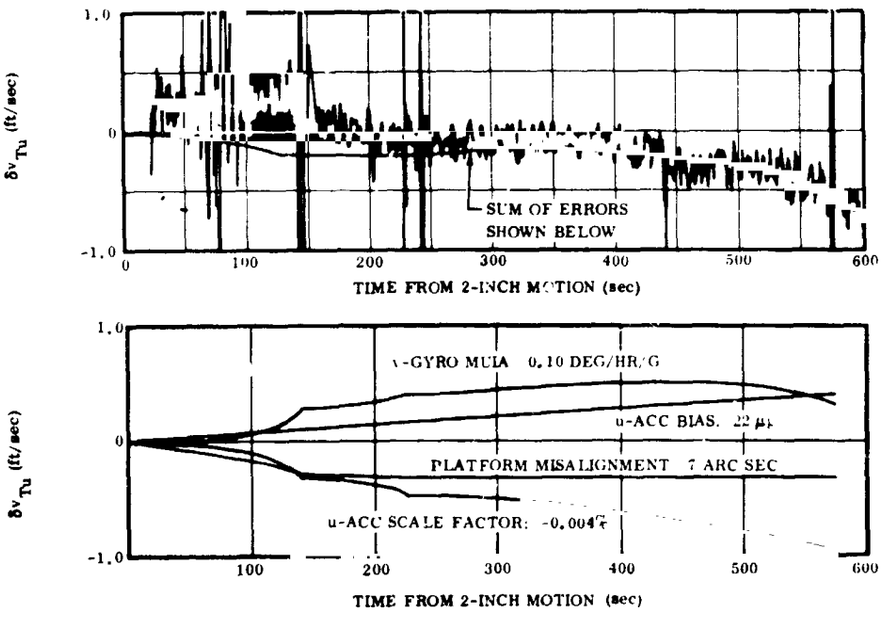

Figure 6-1. u-Error Separation

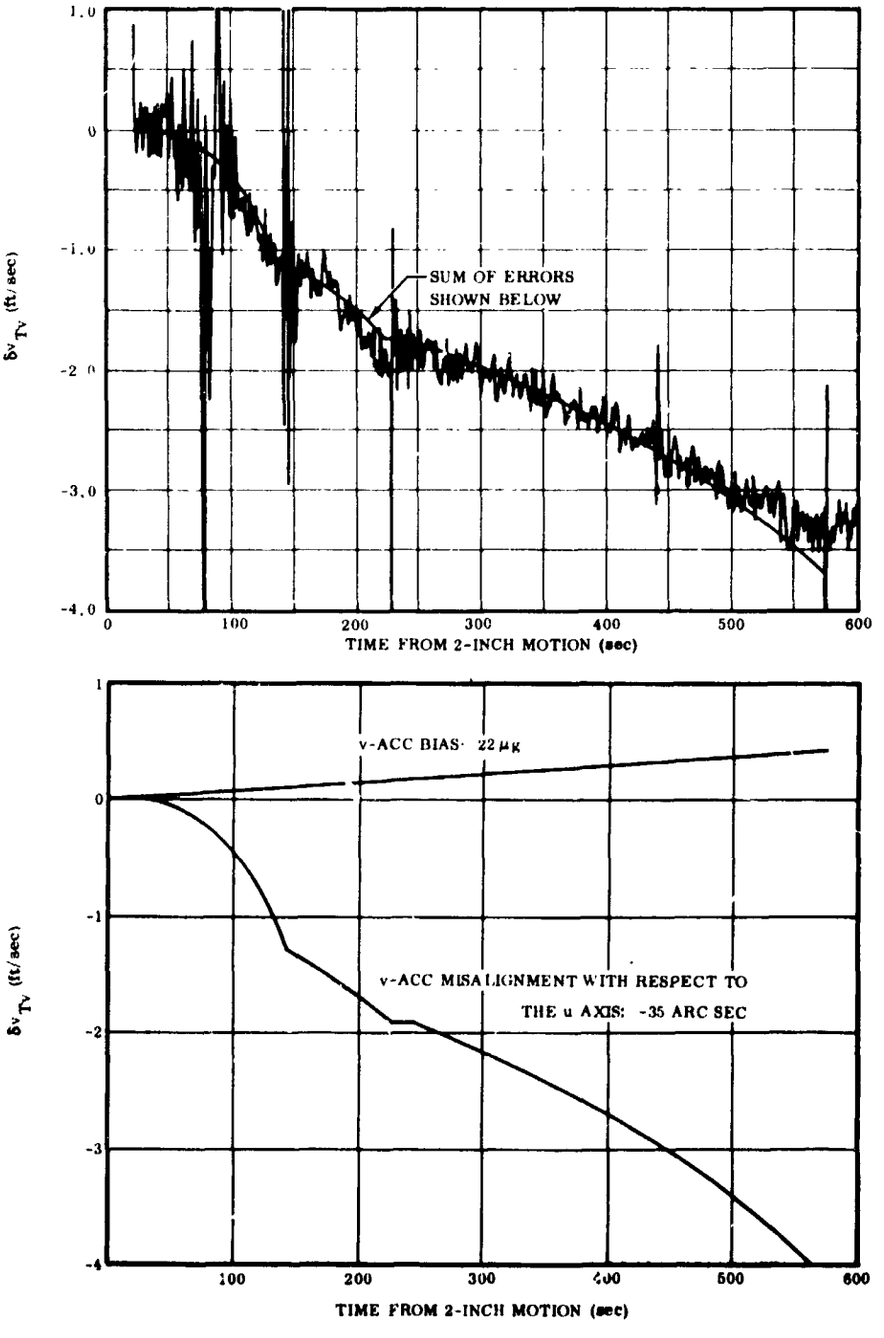

Figure 6-2. v-Error Separation

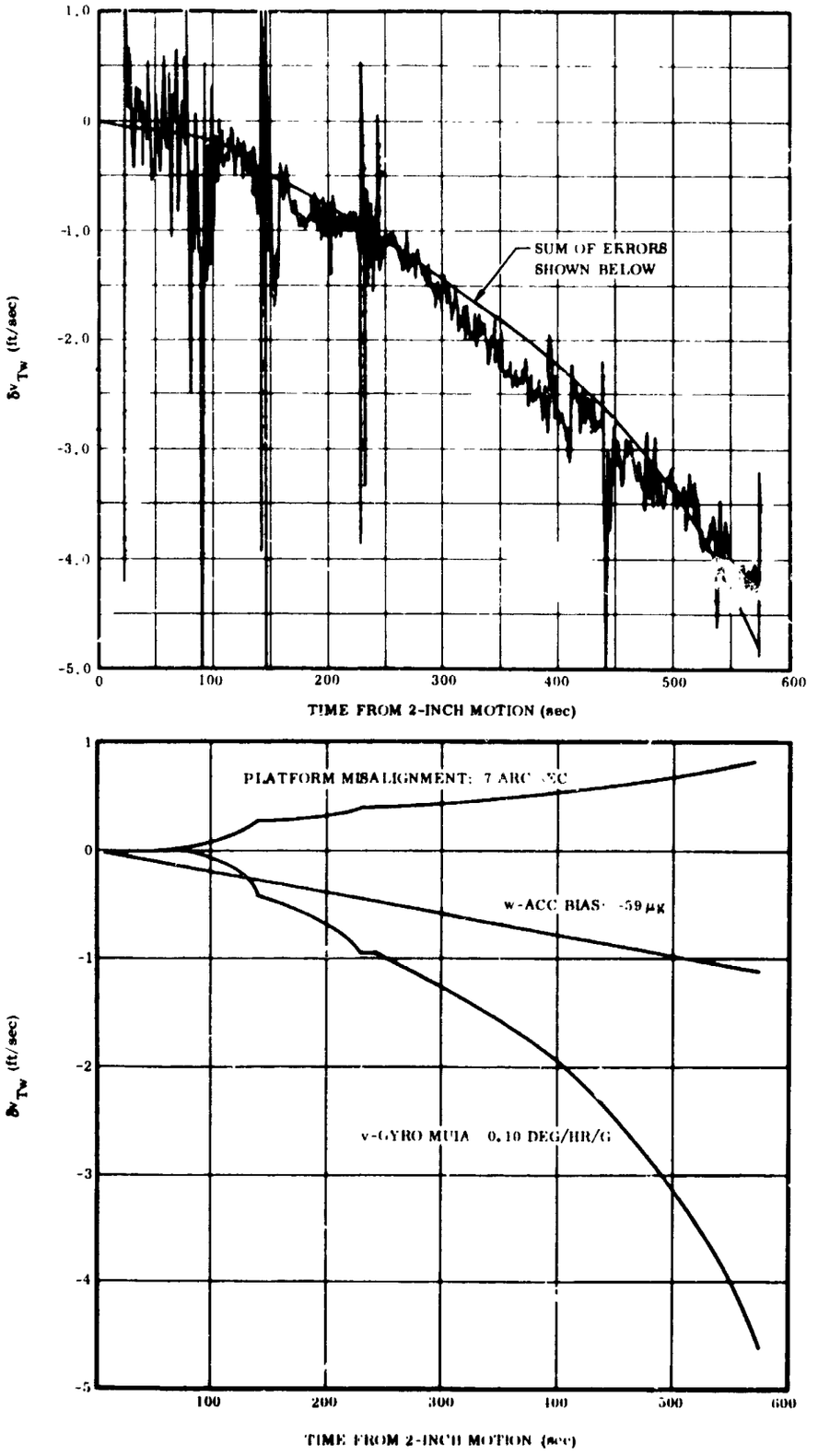

Figure 6-3. w-Error Separation

SECTION 7

ACCELEROMETER LIMIT CYCLE ANALYSIS

The new type GG177 accelerometers were flown on the AC-8 inertial platform. They are of the cantilever type which are maintained in the null position by a series of torquing pulses with a frequency of 3600 per second. These pulses are telemetered as positive or negative, lepending on the direction of the applied torque. The ratio of the number of consecutive positive pulses to the number of consecutive negative pulses immediately following is defined as a limit cycle. A 4/2 limit cycle, for example, means that four positive pulses were followed by two negative pulses. (Under zero-g conditions, the limit cycle ratio should be unity since the accelerometer should be torqued equally in both directions.) The difference between the positive and negative pulses multiplied by 0.1 and the accelerometer scale factor indicates the vehicle's velocity change in feet per second. The acceleration is determined by dividing the velocity change by the elapsed time of the limit cycle pulse sequence.

7.1 LIMIT CYCLE RESULTS. The AC-8 merged and individual Δv pulse telemetry tapes were put through a program that displays the limit cycles in histogram form, as a matrix array of the limit cycles. These histograms are printed out to span various time intervals during flight. Table 7-1 includes a list of the flight intervals considered as well as the limit cycles that occurred. Numbers within each limit cycle column are the percentage frequencies of occurrence of that particular limit cycle out of all the limit cycles that occurred in the corresponding time interval.

During all phases of flight the accelerometers exhibited fewer different limit cycles than any previous flight. In fact, most time intervals exhibited 3/2, 2/2, and 2/3 limit cycles only. The absence of 3/3 or higher limit cycles indicates satisfactory accelerometer loop performance.

In Table 7-1, the first interval of eight seconds covers the time period from computer initialization to about 1/5 second prior to liftoff. This is essentially a 1-g field in the w direction and is represented as such.

The next interval of two seconds covers engine ignition and thrust buildup past flight T_0 (2-inch motion).

The next four intervals represent increases in thrust level prior to BECO. Reflected is the increase of positive limit cycle percentages in each velocity component direction. Most of the change is in the u and w directions with a small increase in the v direction due to the trajectory being north of the u-w plane by 12.0 degrees.

Table 7-1. Limit Cycle History

EVENT	COMPUTER TIME (sec)	PERCENTAGE FREQUENCIES OF LIMIT CYCLES												
		U DIRECTION					V DIRECTION				W DIRECTION			
		4/2	3/2	2/2	2/3	OTHER	3/2	2/2	2/3	OTHER	3/2	2/2	2/3	OTHER
Go Inertial	0-8		2.39	95.25	2.36		1.81	96.47	1.72		31.72	68.26	0.01	
Liftoff	8-10		6.43	87.26	6.31		7.09	85.71	7.14	One 3/3	38.97	60.72	0.12	0.18% of 4/2
1 g Increase in Accel.	10-76		13.89	85.55	0.57		3.53	95.86	0.61		50.07	49.93		One 3/1
2 g Increase in Accel.	76-108		61.45	38.55			10.58	89.42			59.31	40.69		
3 g Increase in Accel.	108-130	18.40	80.71	0.88			17.98	82.02			63.92	36.08		
4.7 g Increase in Accel.	130-150	64.02	24.52			9.29% of 4/1, 2.12% of 5/2, 0.05% of 3/1	26.97	73.03			72.85	27.15		
BECO	150-151	15.36	41.06	4.43		27.47% of 4/1, 10.49% of 5/2, 1.18% of 3/1	29.51	70.49			69.93	30.07		
Sustainer	151-236		46.37	53.61		Three 4/2	8.02	91.96	0.02		10.44	89.55	0.01	
SECO	236-237		61.57	38.43			10.62	89.38			9.34	90 66		
Coast	237-249		5.66	92.98	1.33		2.06	96.73	1.19	One 1/1 and One 2/1	1.86	96.99	1.13	One 2/1, One 2/4 and One 1/3
Main Engine Start	249-250		1.68	97.42	0.90		1.57	96.97	1.46		1.23	97.65	1.12	
1 g Increase in Accel.	250-352		29.04	70.94	0.02		5.46	94.52			3.85	96.12		
2.1 g Increase in Accel.	352-582		48.14	51.85	0.01		9.14	90.85			0.97	96.45	2.53	
First MECO	582-583		75.40	24.60			13.94	86.06				92.40	7.60	
100-lb Thrust "Coast"	583-683		2.31	96.21	1.48		1.45	97.32	1.23		0.98	97.91	1.11	
6-lb Thrust "Coast"	683-1618		1.62	96.80	1.58	One 4/2	1.34	97.38	1.28	One 2/5	1.00	97.98	1.02	One 2/4
6-lb Thrust "Coast"	1618-1728		1.66	96.63	1.71		1.35	97.30	1.35		1.05	97.84	1.11	
6-lb Thrust "Coast"	1728-2038		1.63	96.78	1.59		1.34	97.38	1.28		0.94	98.10	0.96	
100-lb Thrust "Coast"	2038-2082		1.43	97.08	1.48		1.29	97.46	1.25		0.94	97.97	1.09	
Centaur 2nd Burn	2082-2100		4.41	87.21	8.37	One 1/3	4.78	88.42	6.80		4.66	87.05	8.29	
Centaur 2nd Burn	2100-2177		2.20	95.92	1.88		2.07	96.25	1.68		1.48	96.52	2.00	
Coast	2177-2254		1.26	97.49	1.25		1.10	97.82	1.08		0.84	98.33	0.83	
	g LEVEL	4.09	2.46	0	-2.46		2.46	0	-2.46		2.46	0	-2.46	

The pitch program started at 23 seconds (computer time) pitching the vehicle past 45 degrees at 93 seconds. The limit cycle percentages in the u and w directions are approximately equal during the interval containing this time.

Like AC-6, The accelerometers exhibited little sensitivity to vibration during insulation panel jettison and nose fairing jettison.

The period from 1618 seconds to 1728 seconds showed a comparatively large percentage of 2/3 pulses. During this period the analog data indicated that two V engines (50 pounds thrust each) came on four times.

The final period, during the 6-pound thrust period, 1728 to 2038 seconds, showed no evidence of anything unusual having occurred although the V engines supposedly were on seven times.

7.2 Δv PULSE NOISE. The program that generates the histograms also calculates the thrust velocity by accumulating Δv pulses. A first- or second-degree polynomial is fitted over 10 or 20 velocity points by the least-squares method to form one filtered thrust velocity point every one or two seconds. The standard deviation about this point is calculated. This gives a measure of the scattering of data points around the curve fit over a particular interval. A large value indicates that points are more widely scattered. This scattering may be due to accelerometer noise, vehicle vibration, truncation of limit cycles, or a poor curve fit caused by acceleration discontinuities. The telemetered AC-8 flight data displayed a standard deviation greater than 0.1 ft/sec only at the times shown in Table 7-2. Therefore it is concluded that the AC-8 accelerometer data was as noise free as the AC-4 and AC-6 data.

Table 7-2. Times of Large Standard Deviations (>0.1)

DIRECTION	STANDARD DEVIATION (ft/sec)		
	BECO	SECO	FIRST MES
u	0.86	0.41	0.26
v	0.02	0.08	0.05
w	0.36	0.07	0.09

SECTION 8

ANALOG MEASUREMENTS

The following analog measurements relating to guidance system performance were telemetered during the flight:

a. Gimbal servo loop demodulator outputs and d-c torque motor inputs.

b. Gyro torquer voltages.

c. Resolver chain input and output voltages.

d. Accelerometer loop demodulator outputs.

e. Guidance component skin temperatures and platform gyro and accelerometer temperature control amplifier (TCA) outputs.

Plots of these quantities together with an analysis of the data are given in GD/C-BNZ66-026, Atlas/Centaur Flight Evaluation Report, AC-8. A summary of that analysis is given in the following paragraphs.

8.1 PLATFORM GIMBAL SERVO LOOPS. Measurements of the platform gimbal servo loops indicated the inertial reference was maintained throughout the period for which data were acquired with the possible exception of the second MES transient when vehicle angular rates and accelerations were very high.

During booster stage, Gimbal No. 4 uncaged after the vehicle pitched over approximately 18 degrees. This is within the specification of 20 ± 5 degrees.

The maximum gimbal displacement error during flight for Gimbal No. 1 was 6.5 arc seconds; for Gimbal No. 2, 9.2 arc seconds; and for Gimbal No. 3, 12.7 arc seconds. These are all within the dynamic accuracy specification of 60 arc seconds.

At second MES, the inertial pitchover angle of the vehicle roll axis was believed to be about 212 degrees, while the roll orientation was about 240 degrees clockwise. An average clockwise roll rate of 0.18 deg/sec occurred during the coast phase. After the faulty second main engine firing, the vehicle appeared to tumble end-over-end at a rate of 22 deg/sec.

8.2 GYRO TORQUING LOOPS. The platform gyros were torqued throughout the flight to compensate for fixed torque and mass unbalance drifts. The analog torquing signals were compared with the telemetered digital values from the computer. The

only significant difference was an unexplained shift of 0.9 deg/hr which occurred on the w component at nose fairing jettison. Similar shifts occurred on the AC-4 and AC-6 flights. A shift of this magnitude would cause a v component velocity error buildup from 209 seconds to MECO of approximately 12 ft/sec. No such error showed up on the guidance versus BET velocity comparison; therefore the shift is probably due to telemetry instrumentation.

8.3 RESOLVER CHAIN. The analog values of the steering vector, $\bar{f}^*$, were found to satisfactorily compare with the telemetered digital values from the guidance computer. The X (yaw) and Y (pitch) steering voltage outputs of the resolver chain were maintained close to null throughout the sustainer and Centaur first-burn and coast periods, except when guidance was locked out.

8.4 ACCELEROMETER LOOP. The new GG177 accelerometers appeared to be less sensitive to shock and vibration inputs. Smaller pendulum displacements occurred as compared to AC-6. A maximum of 5 arc seconds was evident at nose fairing jettison.

8.5 SKIN TEMPERATURES AND TCA OUTPUTS. Guidance component skin temperatures and platform gyro and accelerometer TCA outputs indicated the system thermal environment was within the required limits throughout the flight.

SECTION 9

GUIDANCE TELEMETRY COVERAGE

9.1 DIGITAL TELEMETRY COVERAGE. Continuous guidance computer telemetry data were obtained from computer time 0 to 2290 seconds. Except for three periods of data dropout at computer times 1665, 1840, and 1847 seconds, the data were error-free. These data were constructed using the TEL 2, Antigua, Coastal Crusader, Sword Knot, Ascension, Rose Knot, and Pretoria data tapes over the intervals specified in Table 9-1. The coverage of the AC-8 flight was excellent. It included large areas of overlap.

Table 9-1. AC-8 Data Tapes Used in Construction of Continuous Digital Telemetry Tape

DATA TAPE	COMPUTER TIME
TEL 2	0 - 505.06
Antigua	505.06 - 811.88
Coastal Crusader	811.88 - 1019.09
Sword Knot	1019.09 - 1283.42
Ascension	1283.42 - 1630.64
Rose Knot	1630.64 - 1910.66
Pretoria	1910.66 - 2290

A total of four edits were required to make the merged telemetry tape error-free (except for the aforementioned dropouts).

Previous Centaur flights have used a ternary telemetry output. AC-8 was the first flight to use a binary (non-return-to-zero) telemetry output with increased signal to noise ratio. The results were excellent.

9.2 Δv PULSE TELEMETRY COVERAGE. An IBM 7094 computer program was used to obtain an error-free Δv pulse telemetry tape. In order to merge out invalid data areas, the program uses three criteria: a) limit-cycle size, b) number of pulses per second, and c) difference in accumulated velocity from computer digital telemetry. Based on a logic table made up of these 3 criteria, the program chooses the best data available.

For AC-8, Δv pulse telemetry covered the same period as the digital telemetry. However, only TEL 2, GBI, and Antigua data tapes were used in the final merged Δv tape. These tapes all contained various periods of invalid data, which has been attributed to telemetry and/or recording errors. TEL 2 was used as the prime tape from computer time 0 to 450 seconds and Antigua was used as the prime tape from 450 to 800 seconds. A number of merges were made in both prime tape sections to substitute good data from a non-prime tape for poor data from the prime tape.

SECTION 10

PREFLIGHT CALIBRATION DATA

10.1 CALIBRATION DATA. This section presents calibration data from 35 separate calibrations of MGS 30 prior to the flight of AC-8. The calibration data are shown in Figures 10-1 through 10-6. The date and location of each calibration is indicated in the figure. Where dates are shown connected, calibrations were performed consecutively, without a shutdown. The circled values are the final calibration values that were used during flight. The specification shift values from Convair Report 55-04040, Revision F, are also shown on the curves.

The last calibrated value of d_9 was adjusted to account for the shift observed when switching to vehicle internal power.

Honeywell calibrations of d_6 are not shown because of a calibration error that produced erroneous values.

10.2 CALIBRATION SHIFTS. The D-value shift between each calibration was determined and the standard deviation computed for the following three sets of data:

a. Calibration shifts with no shutdown.

b. Calibration shifts after shutdown (Site-to-site shifts excluded for D_1, D_2, D_3, d_7, d_8, and d_9).

c. All calibration shifts.

The results are shown in Table 10-1 compared with the acceptance test criteria for Phase I PIP systems. The most significant change from previous data is in the smaller accelerometer scale factor shifts. For example, the average standard deviation of scale factor shift for no shutdown is approximately one-half the value observed on the AC-6 system; MGS 30 contained the improved GG 177 accelerometers. The standard deviation of bias shifts remained approximately the same as in the AC-6 data.

As indicated in the table, all of the gyro-shift sigmas, except for d_{15}, were within both the shutdown and no-shutdown acceptance specifications. Although the sigma for d_{15} was slightly larger, the actual d_{15} shifts never exceeded the acceptance specifications. MGS 30 contained D20 gyros.

Table 10-1. Calibration Shift Standard Deviations

D-VALUE	UNITS	σ (NO SHUTDOWN)		σ (AFTER SHUTDOWN)		σ(ALL CALIB.)	1/3 SPEC**
		CALIB.	1/3 SPEC*	CALIB.	1/3 SPEC*		
D_1	None × 10^{-6}	16	70.0	20	93	26	70
D_2	None × 10^{-6}	23	117.0	22	117	26	150
D_3	None × 10^{-6}	20	70.0	31	93	59	150
d_4	Millirad		0.15	0.10	0.15	0.08	0.15
d_5	Millirad		0.25	.08	0.25	0.07	0.25
d_6	Millirad		0.50		0.50		0.50
d_7	ft/sec^2	0.0011	0.0021	0.0029	0.0029	0.0039	0.0032
d_8	ft/sec^2	0.0005	0.0032	0.0015	0.0033	0.0023	0.0052
d_9	ft/sec^2	0.0008	0.0021	0.0016	0.0029	0.0039	0.0052
d_{10}	deg/hr	0.07	0.12	0.11	0.17	0.10	0.12
d_{13}	deg/hr	0.05	0.08	0.12	0.14	0.10	0.06
d_{16}	deg/hr	0.07	0.12	0.12	0.17	0.11	0.12
d_{11}	deg/hr/g	0.10	0.14	0.13	0.19	0.12	0.30
d_{14}	deg/hr/g	0.08	0.08	0.08	0.14	0.08	0.12
d_{17}	deg/hr/g	0.07	0.14	0.10	0.19	0.10	0.30
d_{12}	deg/hr/g	0.03	0.13	0.05	0.20	0.05	0.21
d_{15}	deg/hr/g	0.14	0.13	0.08	0.20	0.13	0.21
d_{18}	deg/hr/g	0.04	0.13	0.15	0.20	0.15	0.40

* Acceptance Test Procedures for the DVG 8012 MGS, Honeywell Document R-ED 21110 Revision E

** Specification For Vehicleborne Guidance Set, Convair Report No. 55-04040 Revision F

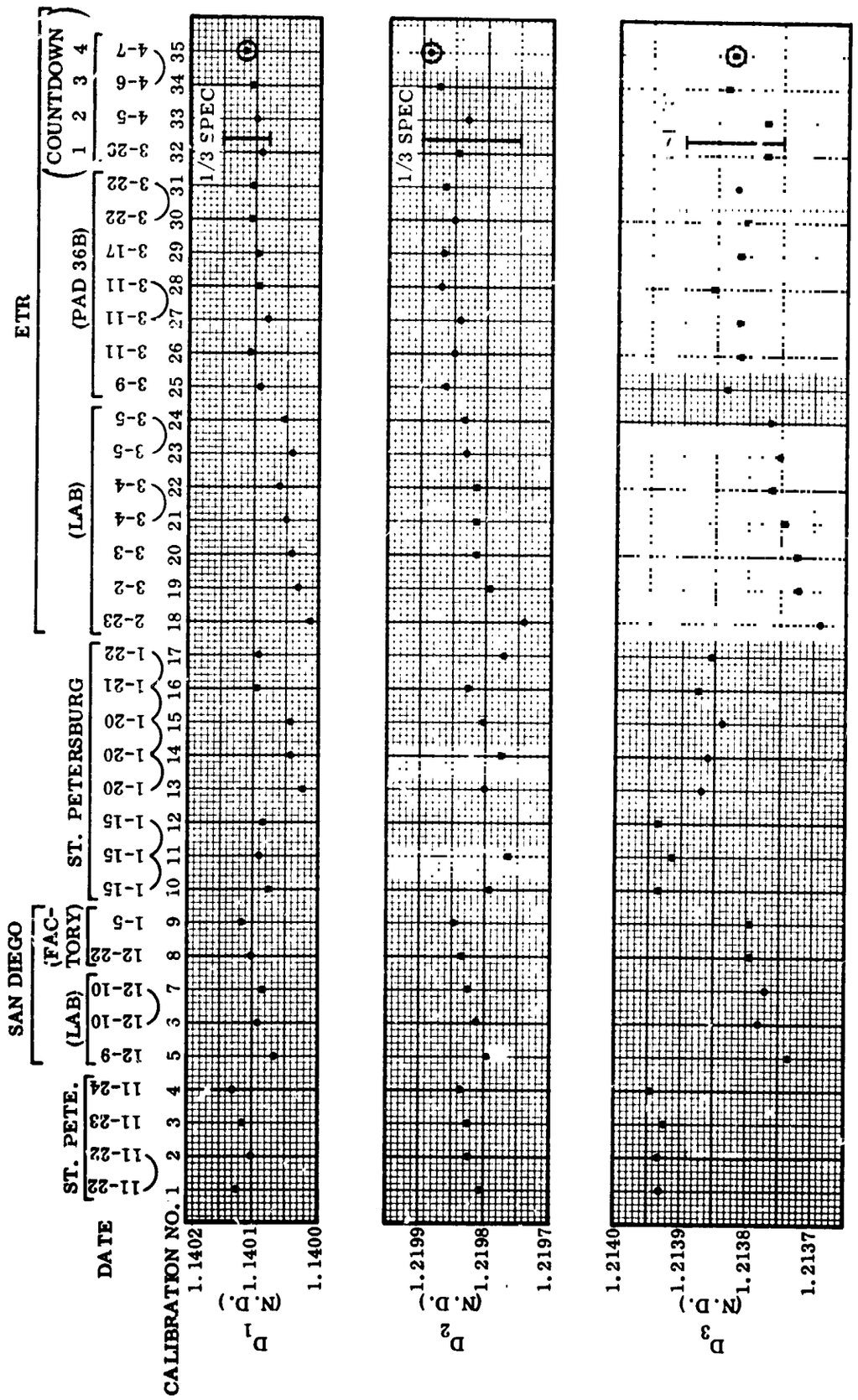

Figure 10-1. Accelerometer Scale Factor

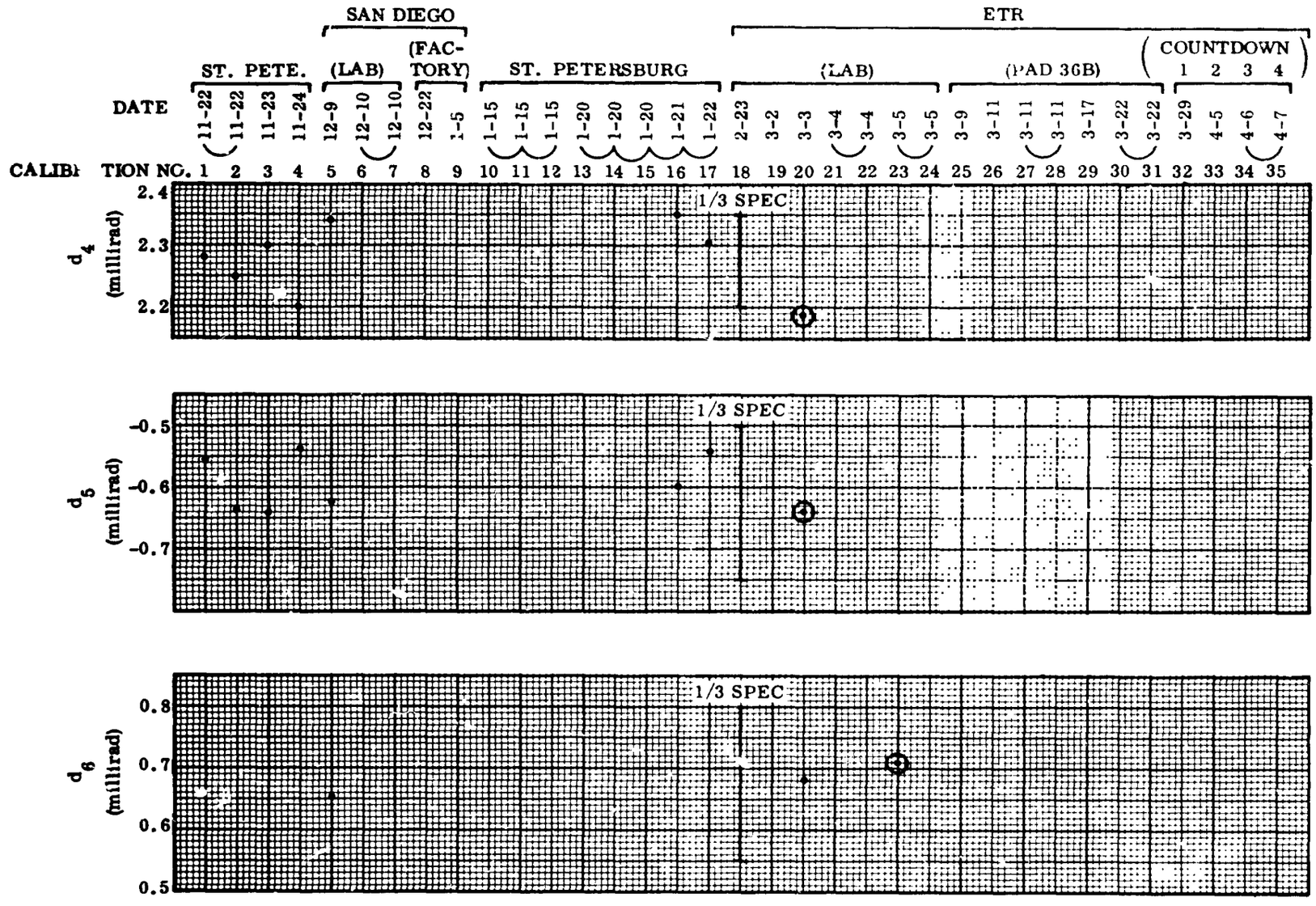

Figure 10-2. Accelerometer Misalignment

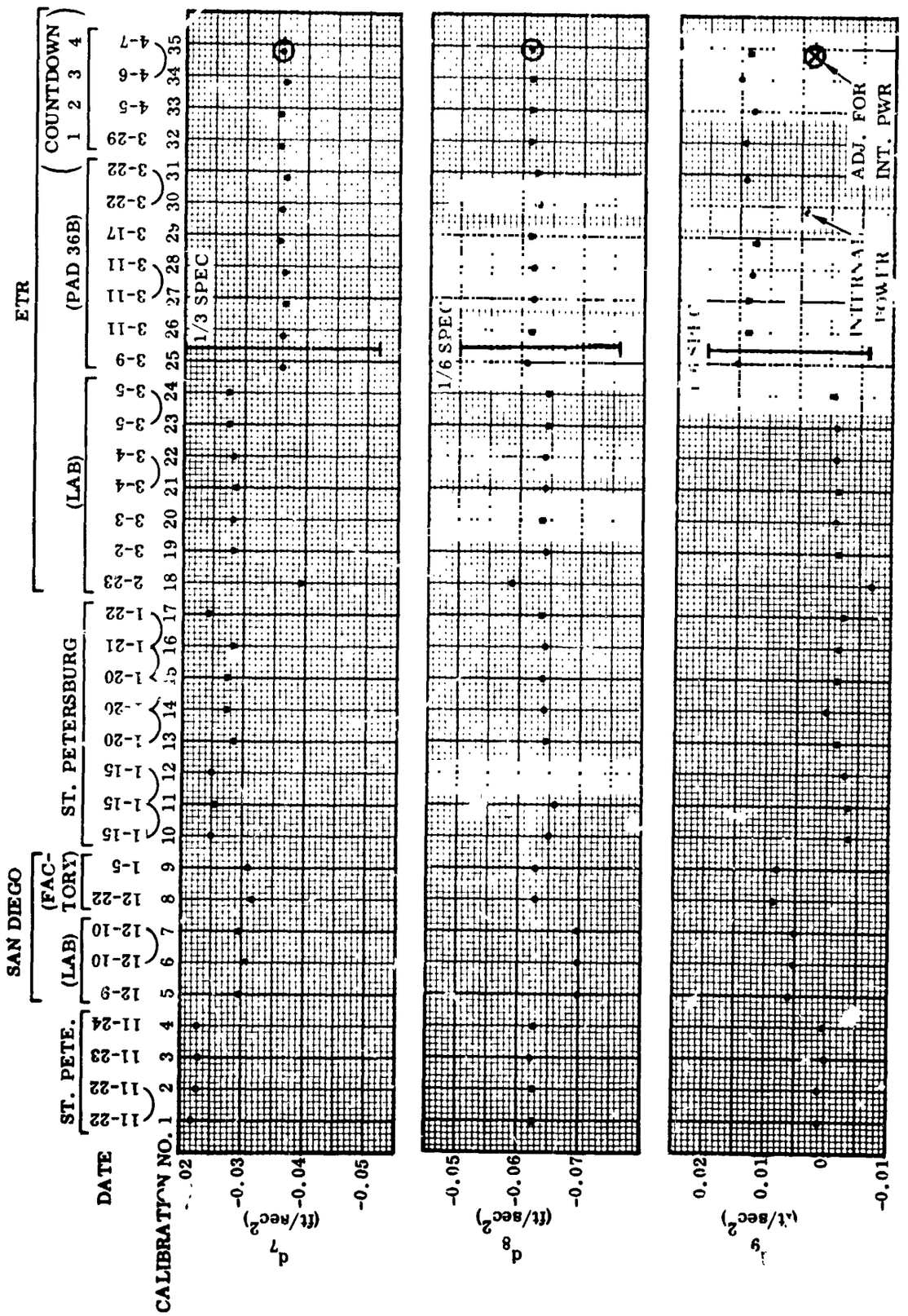

Figure 10-3. Accelerometer Bias

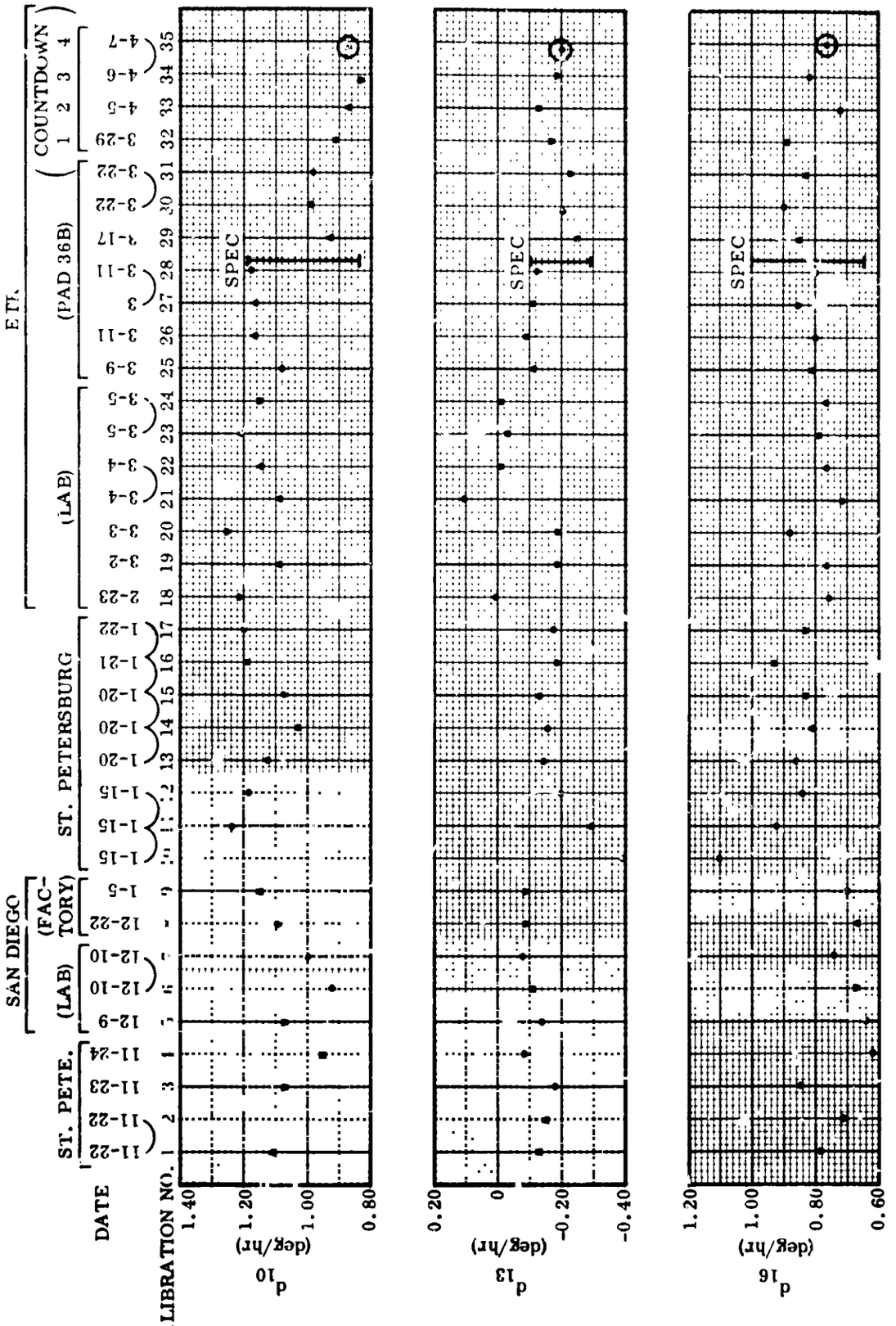

Figure 10-4 Gyro Fixed Torque Drift

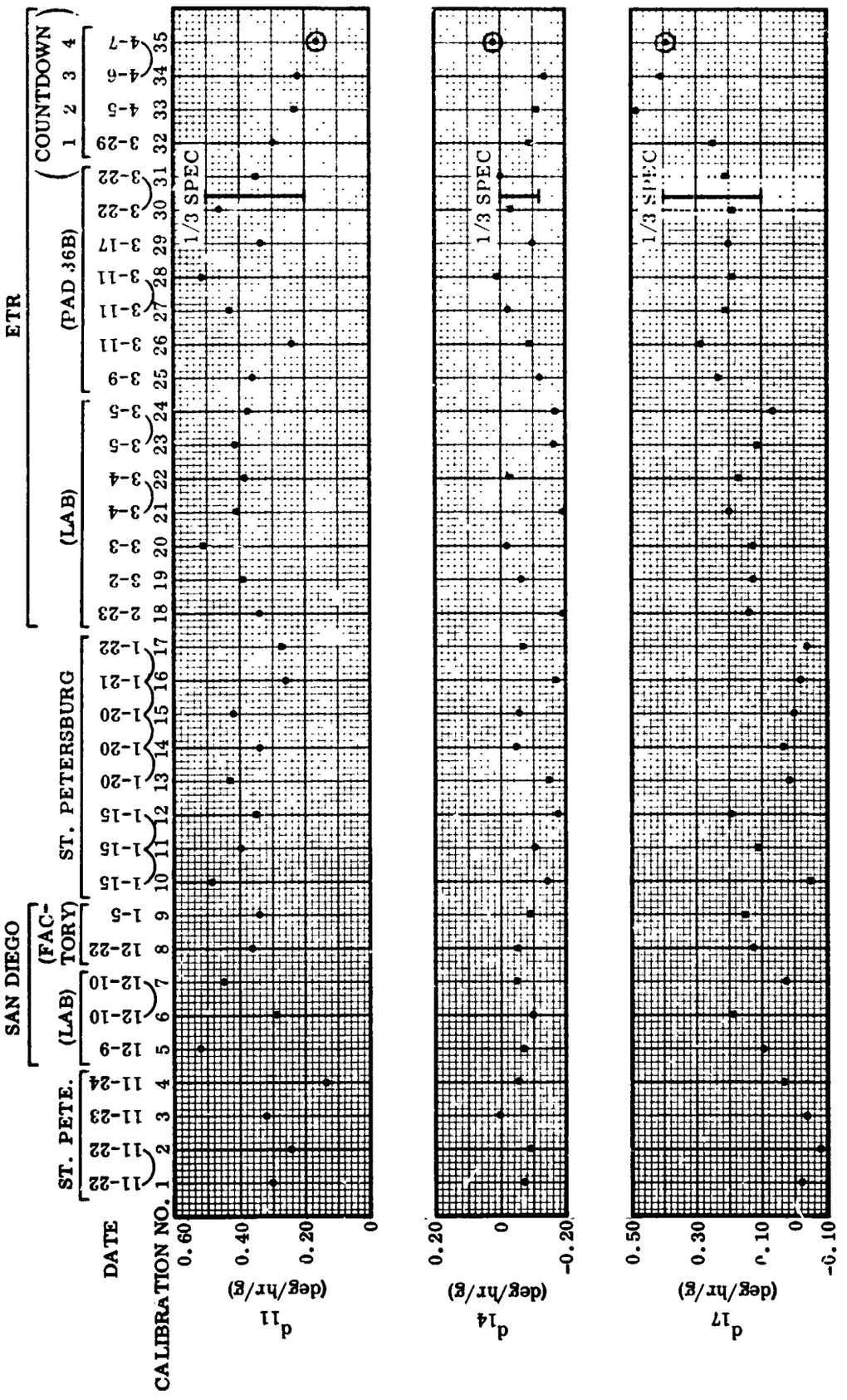

Figure 10-5. Gyro Input Axis Mass Unbalance Drift

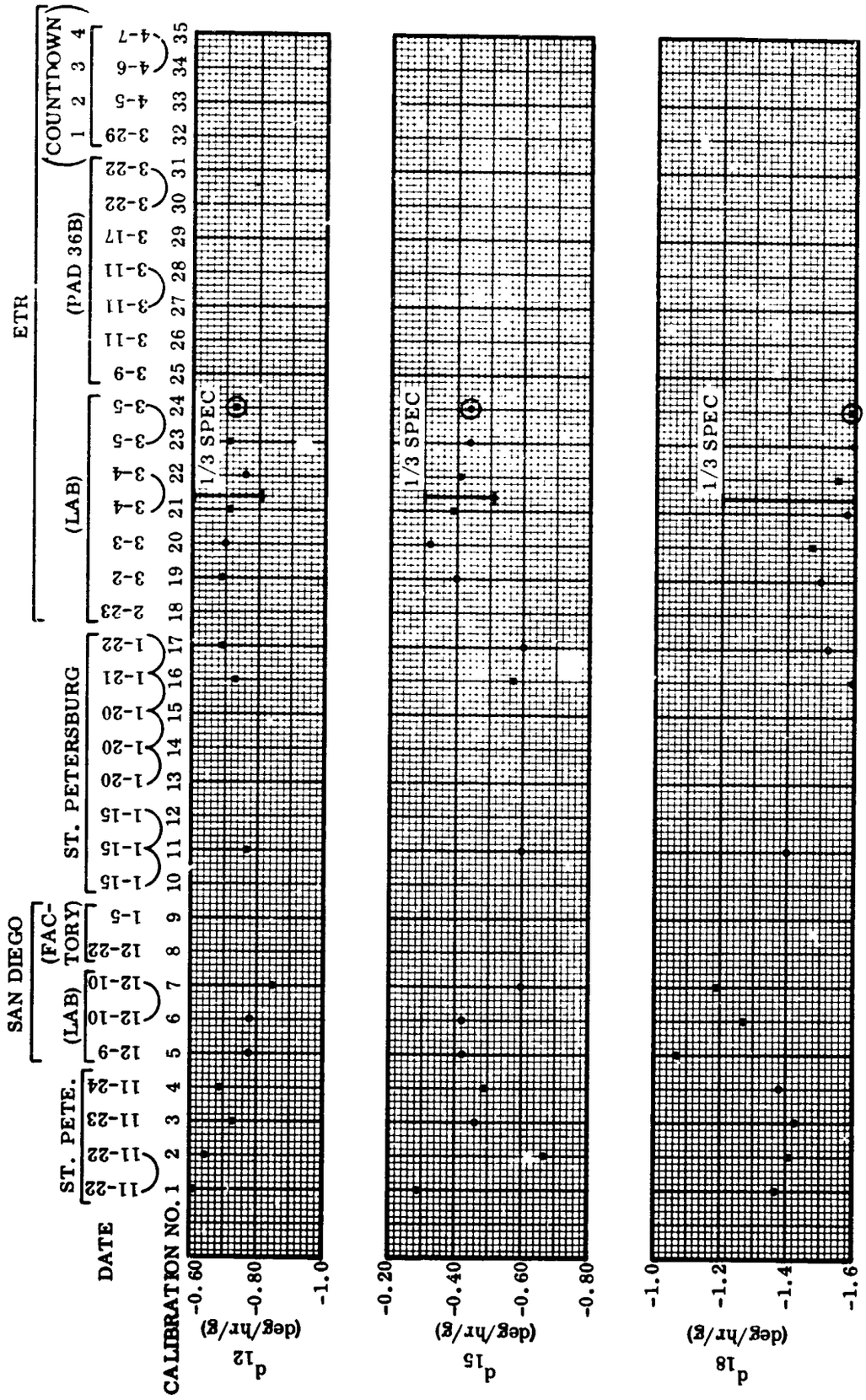

Figure 10-6. Gyro Spin Axis Mass Unbalance Drift

APPENDIX A

FINAL GUIDANCE EQUATION FLOW CHARTS AND CONSTANTS

GUIDANCE INITIALIZATION

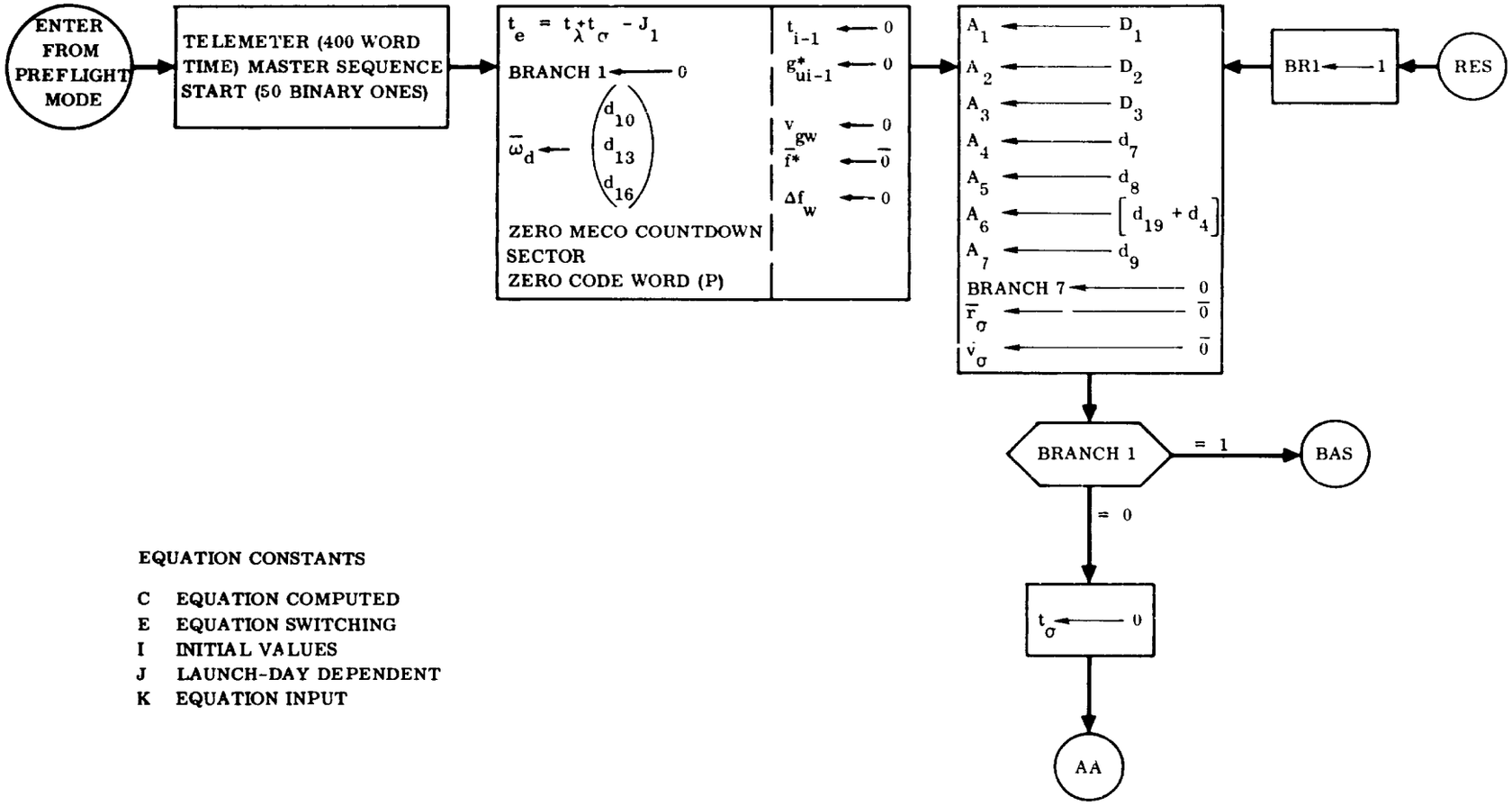

EQUATION CONSTANTS

- C EQUATION COMPUTED
- E EQUATION SWITCHING
- I INITIAL VALUES
- J LAUNCH-DAY DEPENDENT
- K EQUATION INPUT

NOTES: Y ← X = STORE X IN Y LOCATION

Figure A-1. Guidance Initialization

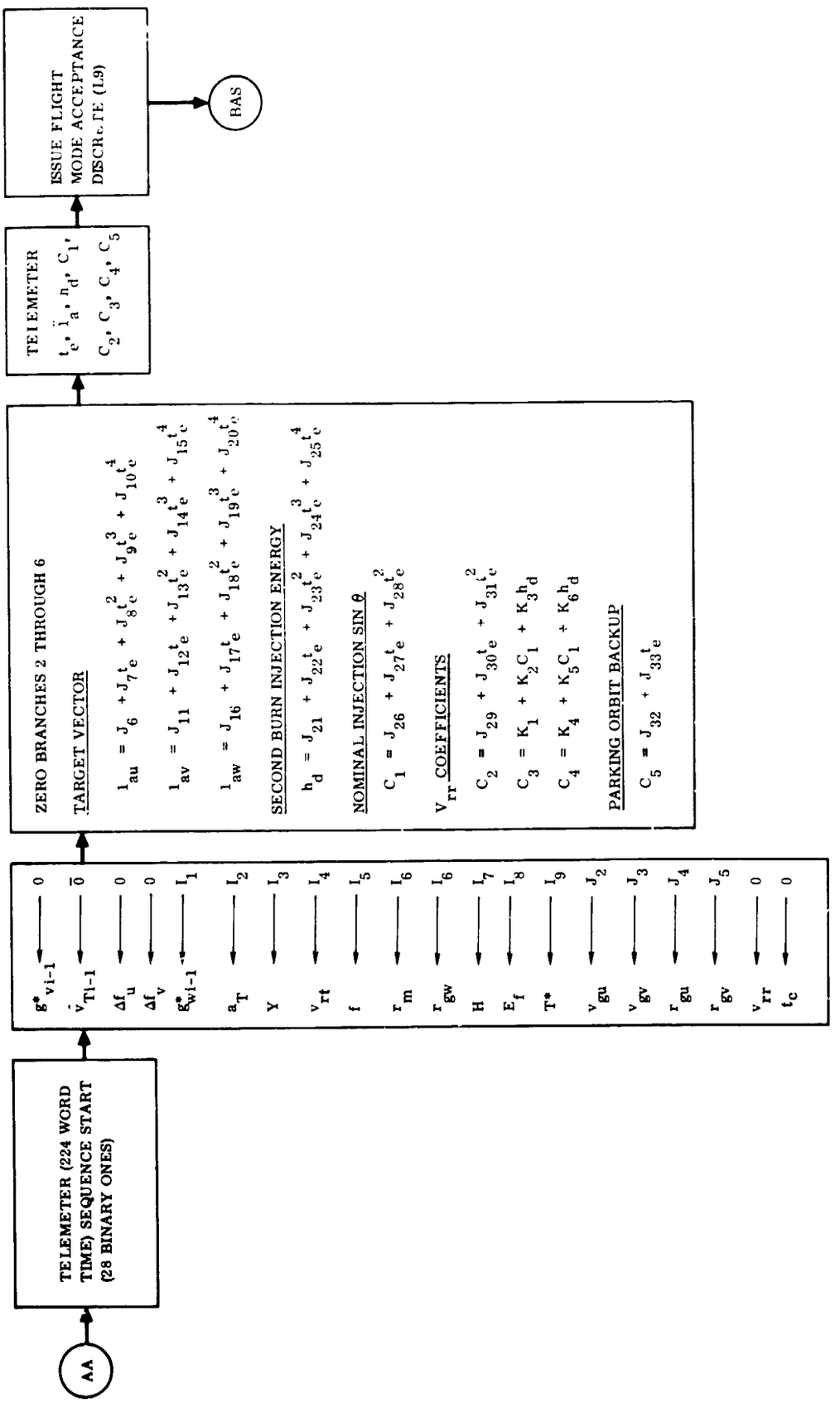

Figure A-2. Inflight Prelaunch

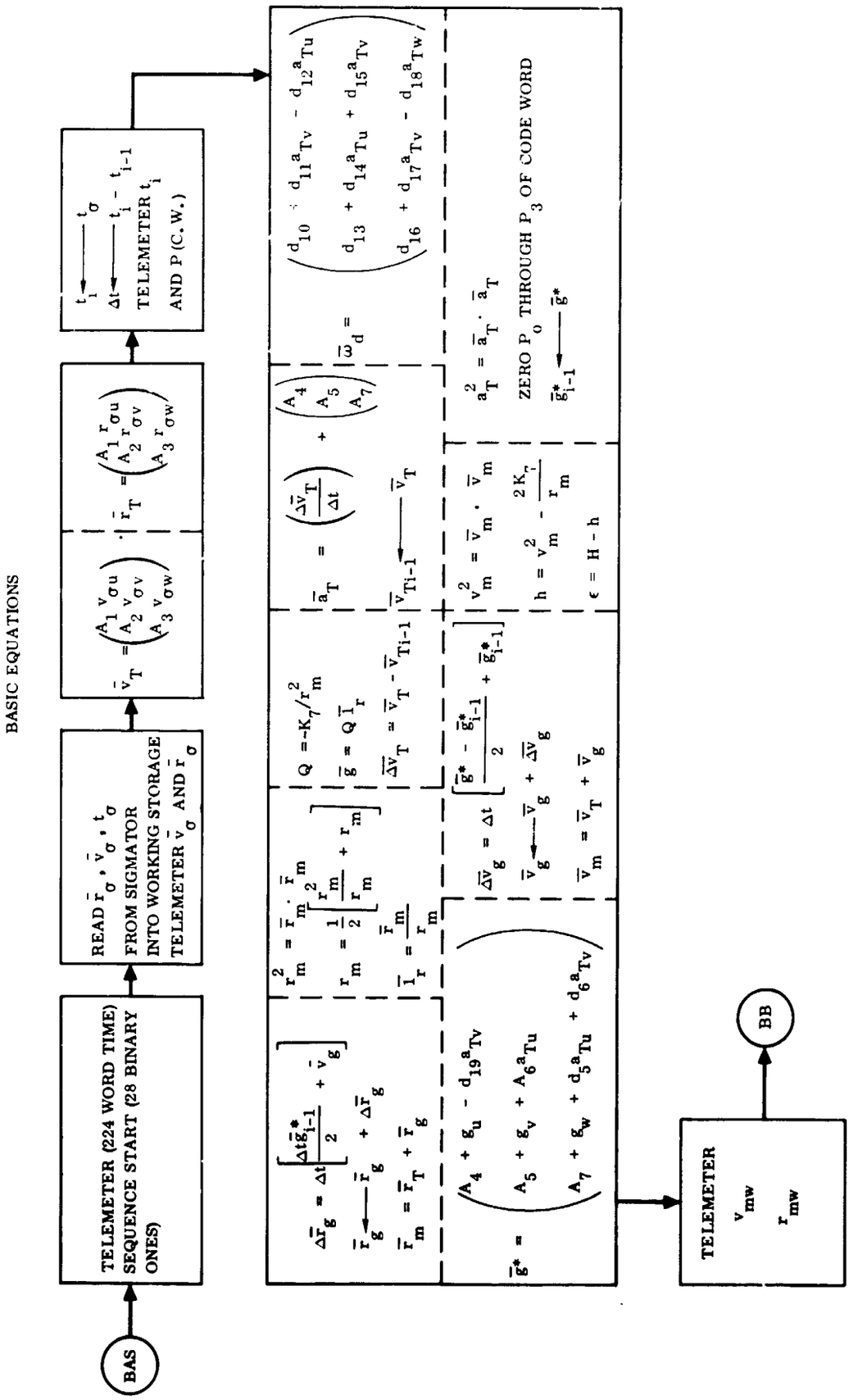

BASIC EQUATIONS

Figure A-3. Basic

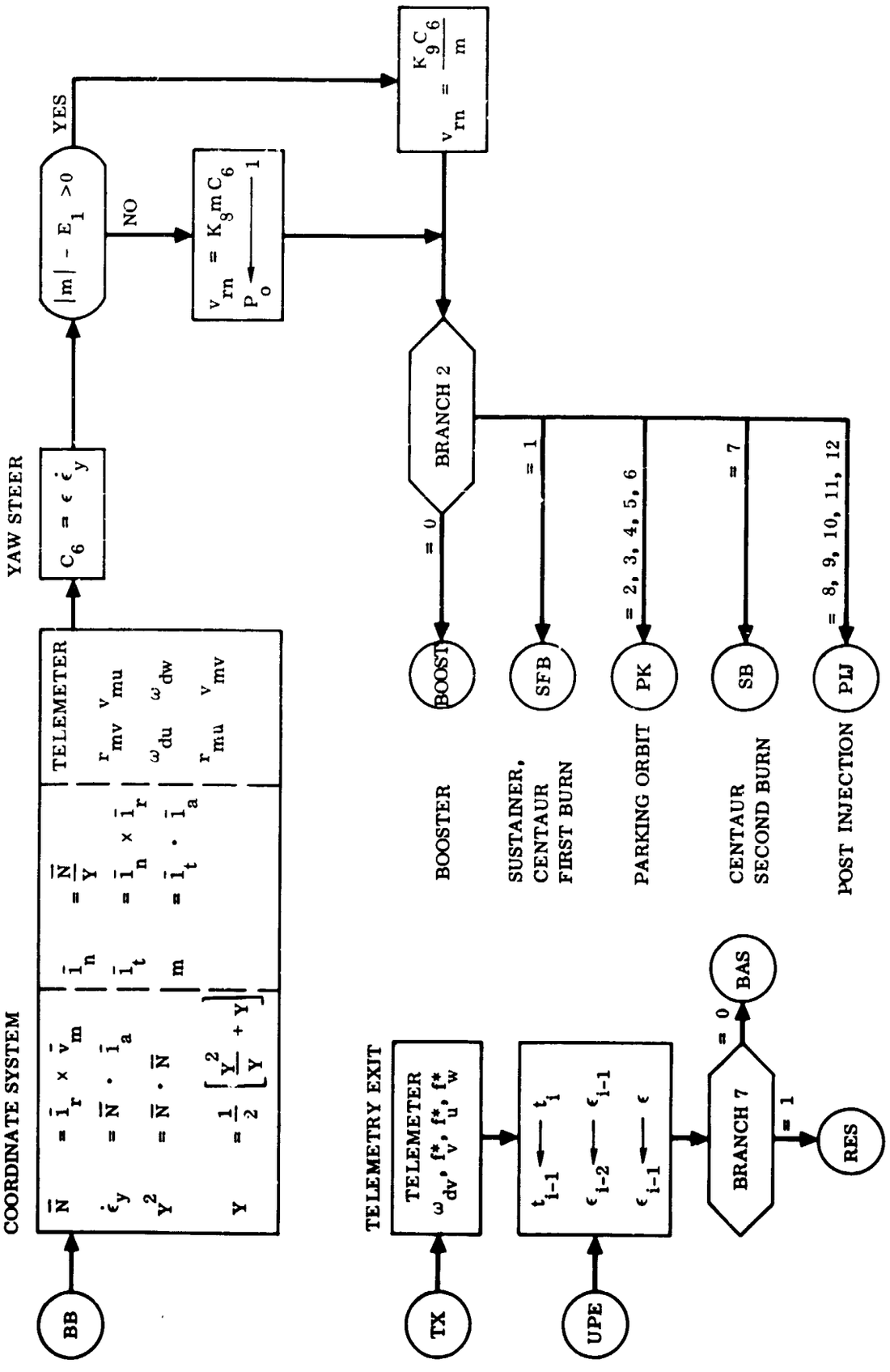

Figure A-4. Coordinate System

BOOSTER EQUATIONS

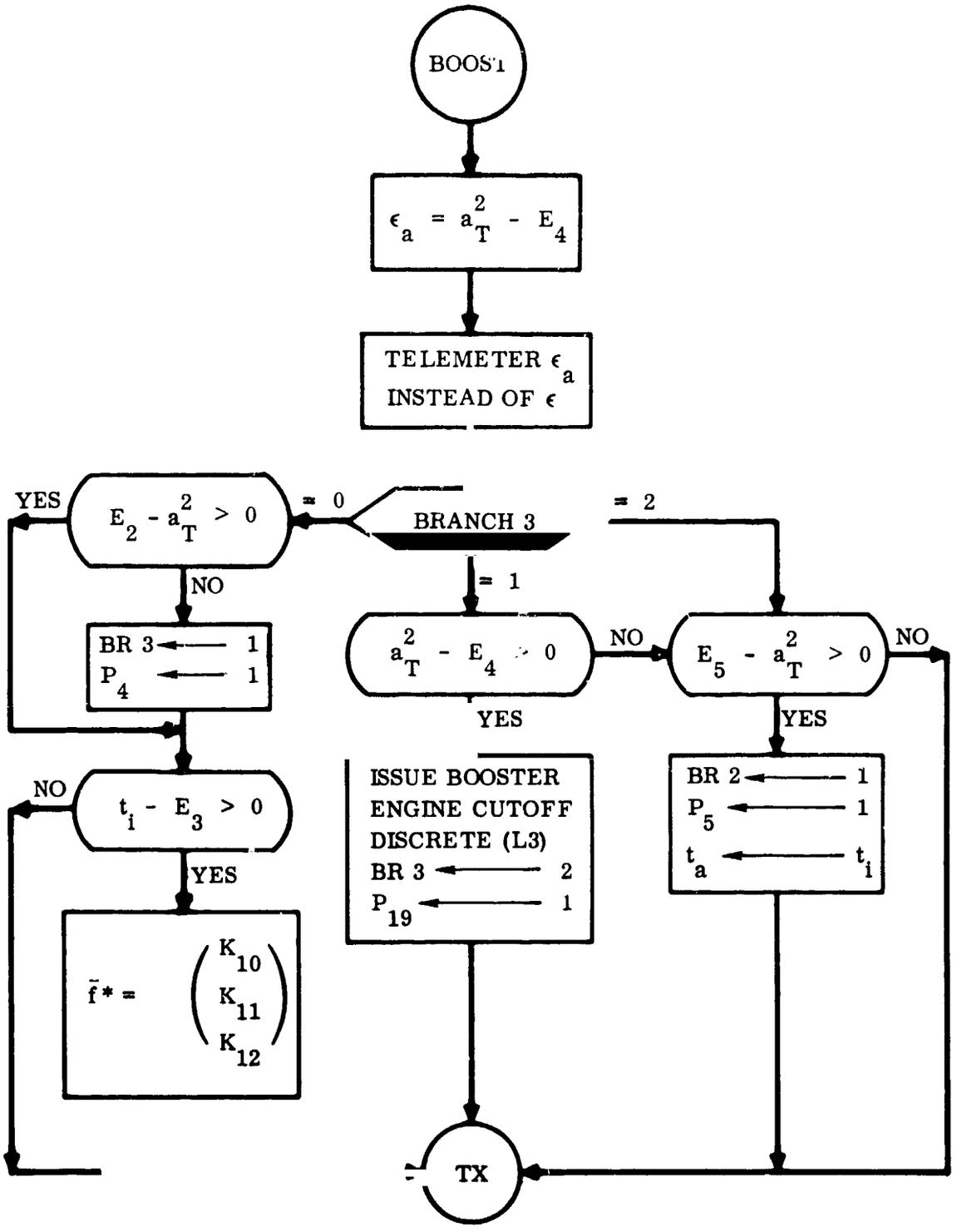

Figure A-5. Booster

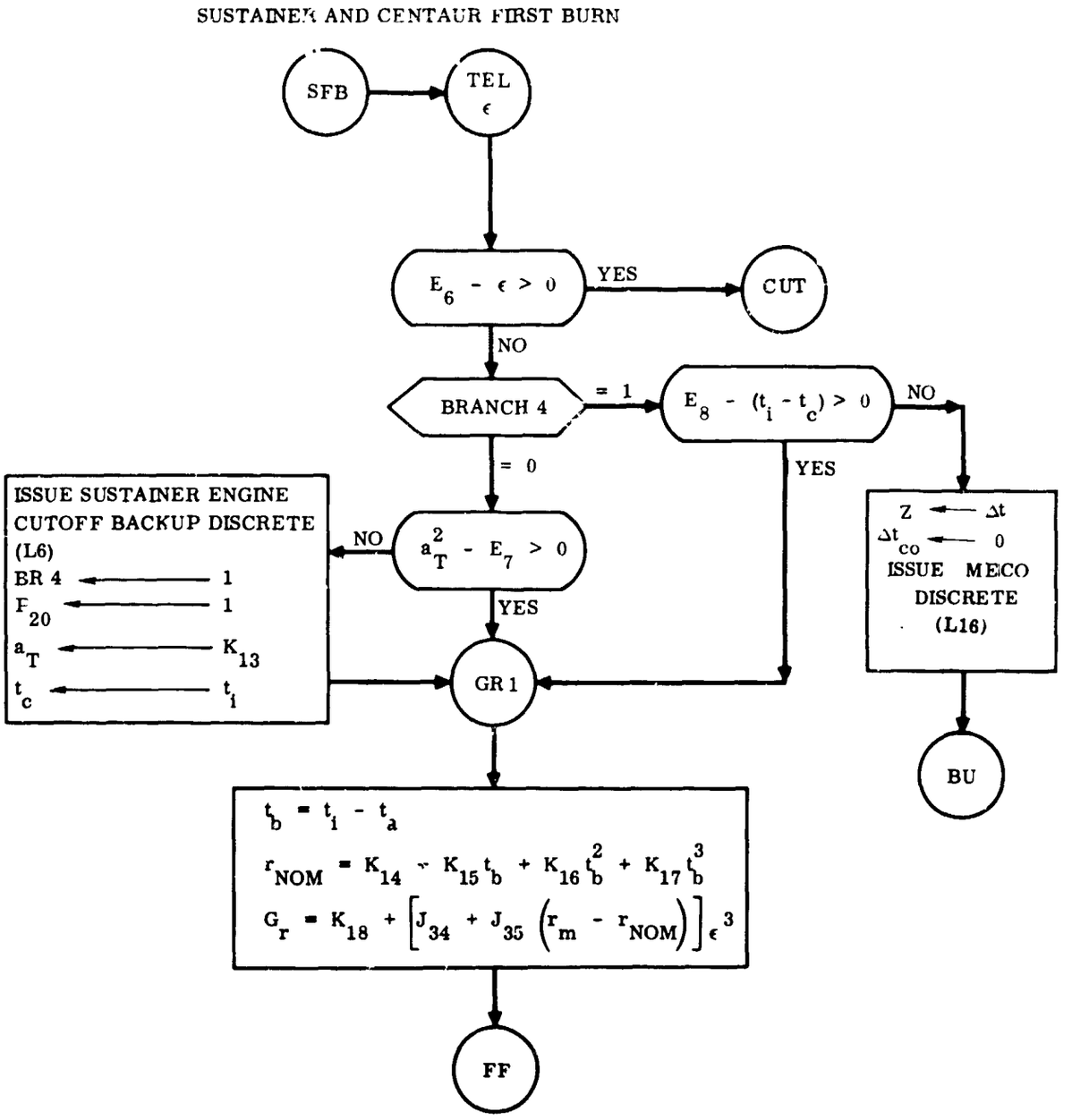

Figure A-6. Sustainer and Centaur First Burn

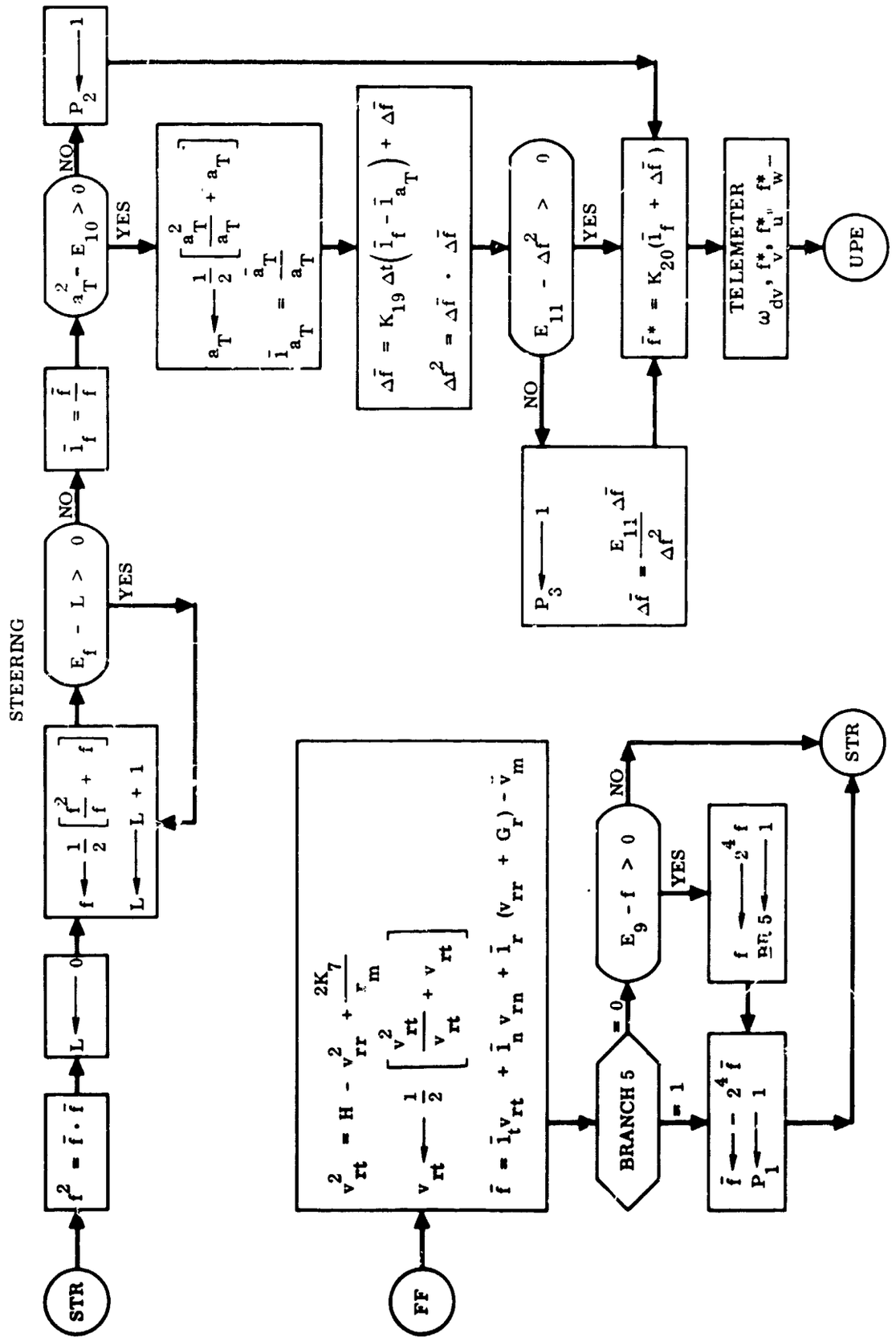

Figure A-7 Steering

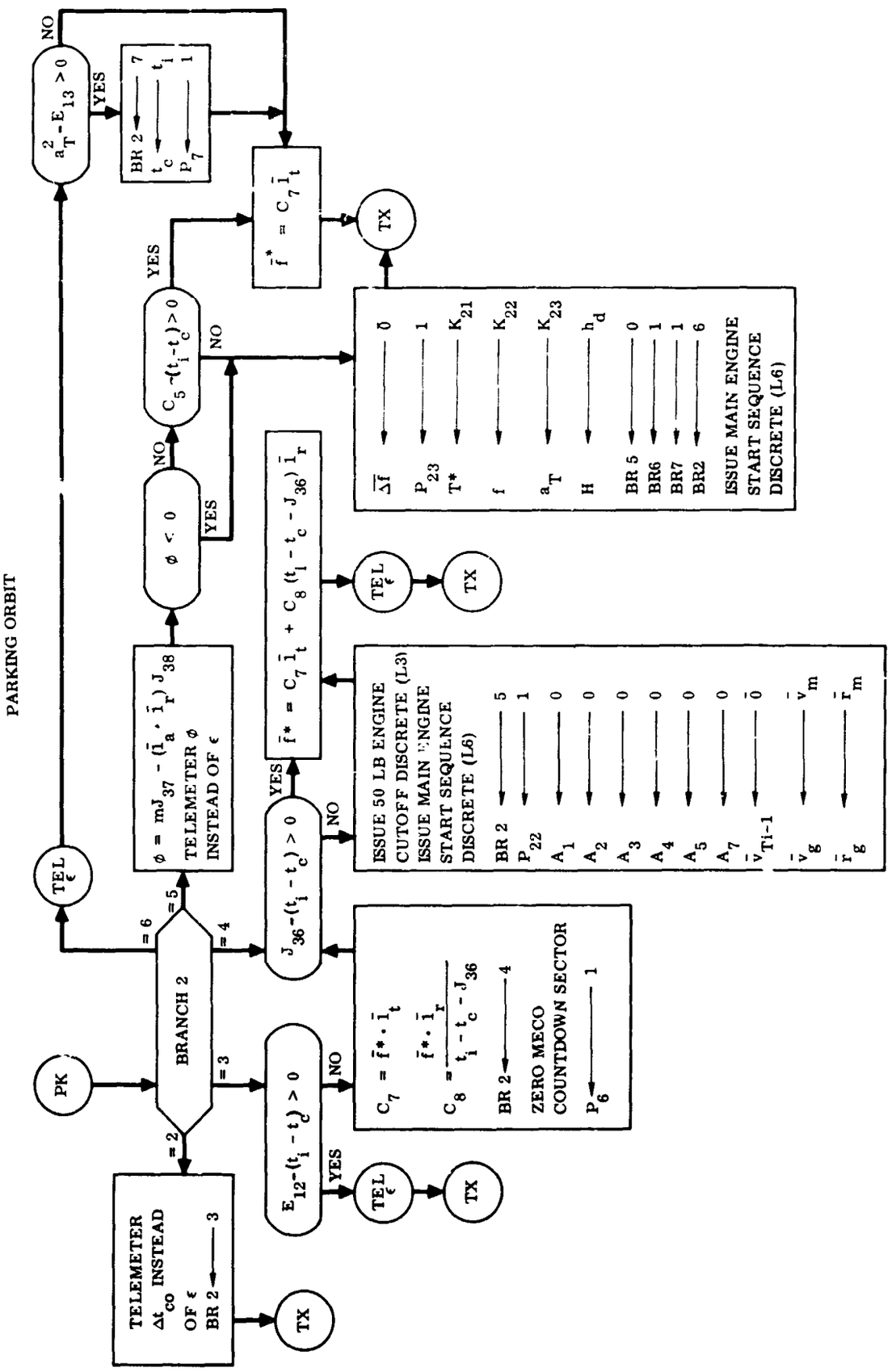

Figure A-3. Parking Orbit

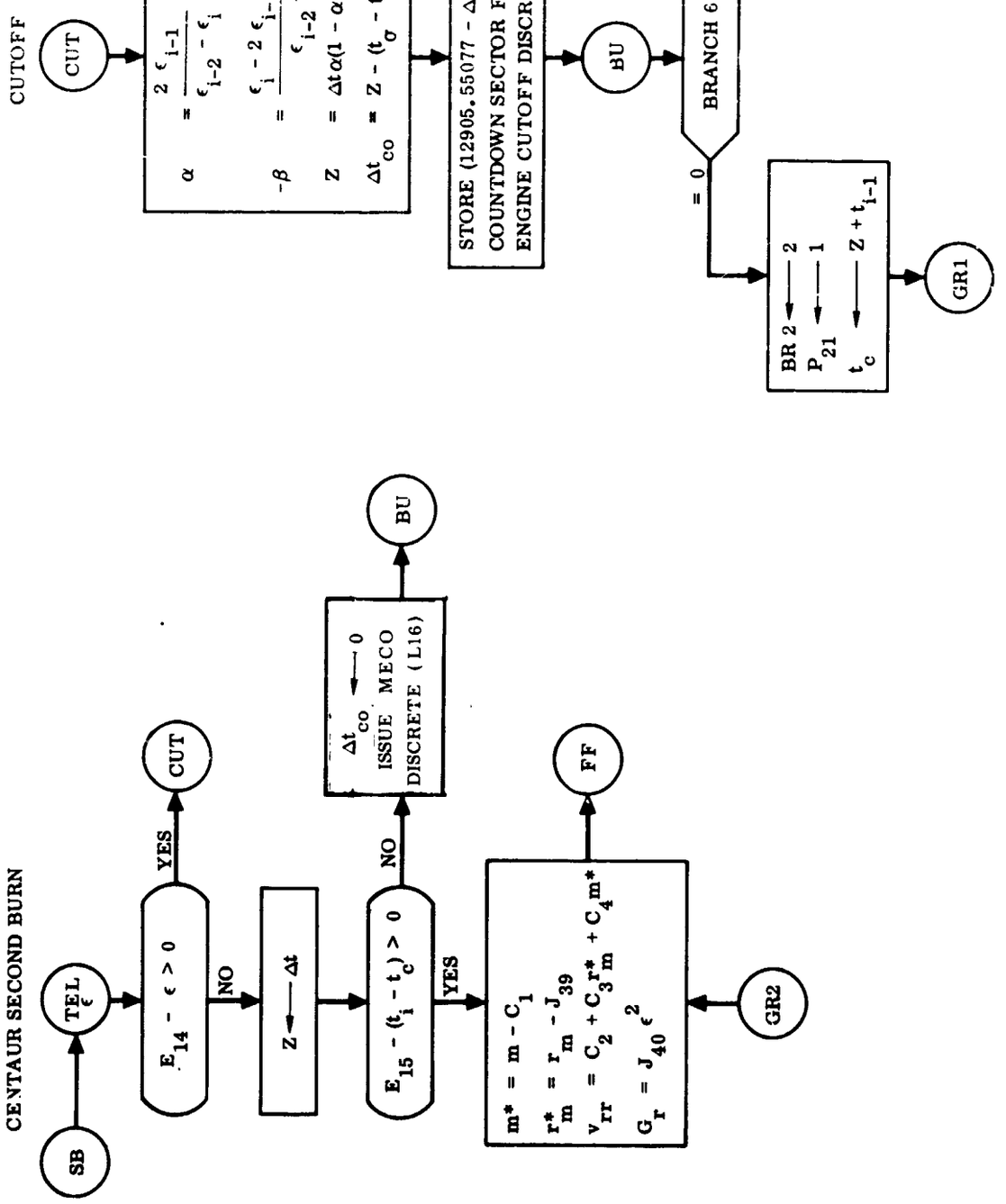

Figure A-9. Centaur Second Burn and Cutoff Extrapolation

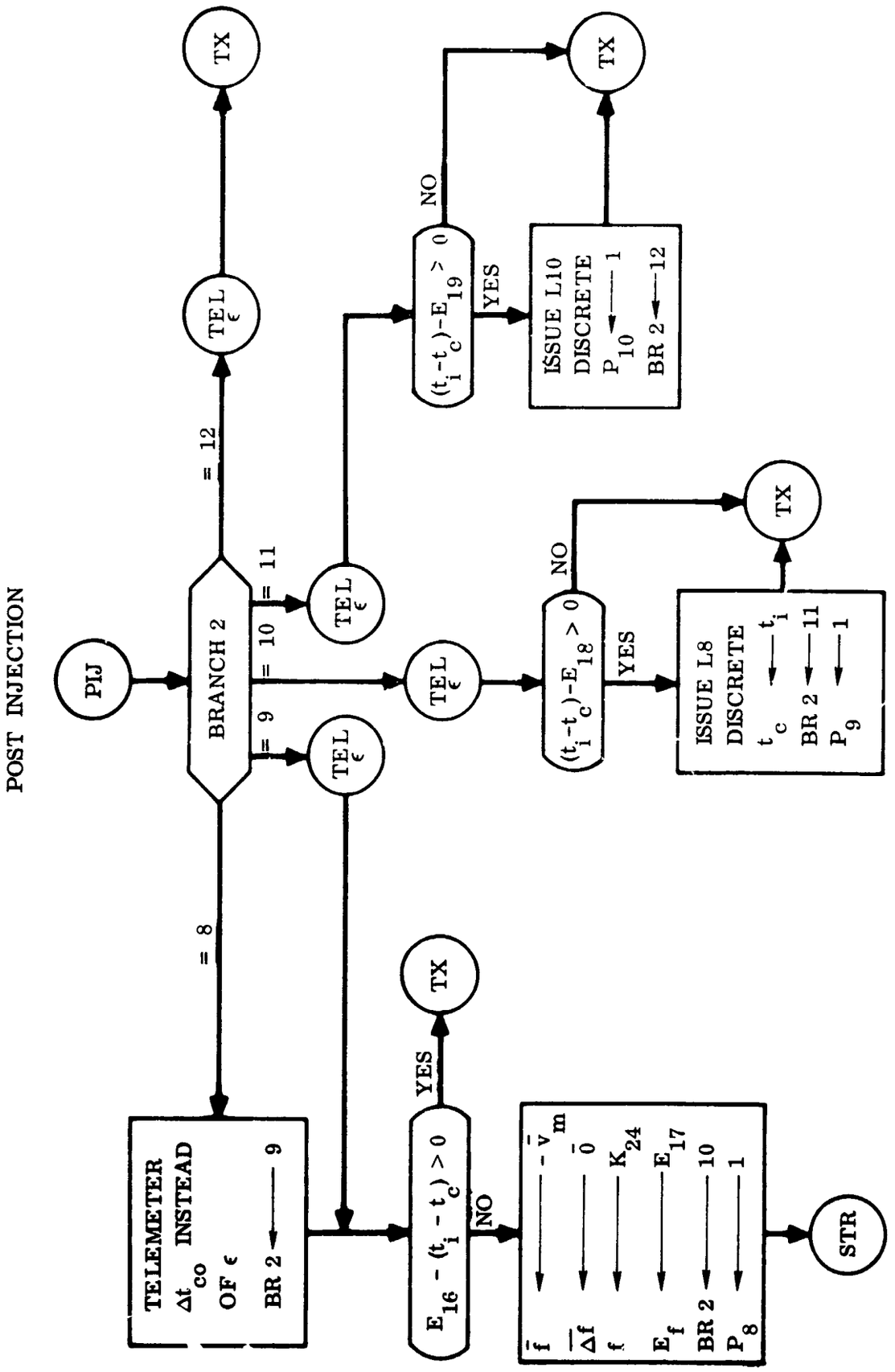

Figure A-10. Post Injection

Table A-1. Calibration Constants

CON-STANT	VALUE	UNITS	SCALE FACTOR	DEFINITION
D_1	0.11401162+01	None	2.0	u, v, w: accelerometer scale factor
D_2	0.12198884+01	None	2.0	
D_3	0.12138254+01	None	2.0	
d_4	0.21867752-02	None	0.125	v input axis misalignment with the u axis
d_5	-0.63563883-03	None	0.125	w input axis misalignment with the u axis
d_6	0.70953369-03	None	0.125	w input axis misalignment with the v axis
d_7	-0.35922527-01	ft/sec^2	65.0	u, v, w: accelerometer bias
d_8	-0.61159730-01	ft/sec^2	65.0	
d_9	0.83297491-02	ft/sec^2	65.0	
d_{10}	0.42049851-05	rad/sec	0.40288016-03	u gyro fixed torque drift
d_{11}	0.24639728-07	rad-sec/ft	0.77476955-06	u gyro drift due to mass unbalance along the input axis
d_{12}	-0.10937760-06	rad-sec/ft	0.77476955-06	u gyro drift due to mass unbalance along the spin reference axis
d_{13}	-0.10187259-05	rad/sec	0.40288016-03	v gyro fixed torque drift
d_{14}	0.25299177-08	rad-sec/ft	0.77476955-06	v gyro drift due to mass unbalance along the input axis
d_{15}	-0.66108923-07	rad-sec/ft	0.77476955-06	v gyro drift due to mass unbalance along the spin reference axis

Table A-1. Calibration Constants, Contd

CON-STANT	VALUE	UNITS	SCALE FACTOR	DEFINITION
d_{16}	0.36950818-05	rad/sec	0.40288016-03	w gyro fixed torque drift
d_{17}	0.58938067-07	rad-sec/ ft	0.77476955-06	w gyro drift due to mass unbalance along input axis
d_{18}	-0.24060231-06	rad-sec/ ft	0.77476955-06	w gyro drift due to mass unbalance along spin reference axis
d_{19}	-0.15185028-02	None	0.125	Misalignment of both the u and v input axis with the u reference axis

Table A-2. Equation Switching Constants

CON-STANT	VALUE	UNITS	SCALE FACTOR	DEFINITION
E_1	0.03	None	2.0	Value of $\|m\|$ to switch to alternate v_{rn} calculation
E_2	$10000.^0$	$(ft/sec^2)^2$	270400.0	BECO enable acceleration
E_3	200	sec	12905.55	Time from $t_\sigma = 0$ for output of $\bar{f}^*$ in booster (for ground check-out)
E_4	30982.0	$(ft/sec^2)^2$	270400.0	BECO acceleration
E_5	2500.0	$(ft/sec^2)^2$	270400.0	Booster-sustainer equation switching acceleration
E_6	0.1×10^8	$(ft/sec)^2$	$0.27487791 \times 10^{10}$	Energy-to-be gained to enter first MECO cutoff computation
E_7	550.0	$(ft/sec^2)^2$	270400.0	SECO backup acceleration
E_8	360.0	sec	12905.55	First MECO time backup
E_9	1500.0	ft/sec	52488.8	Value of f for rescaling $\bar{f}$ computation
E_{10}	550.0	$(ft/sec^2)^2$	270400.0	Minimum value of a_T^2 for computing $\|\bar{a}_T\|$
E_{11}	0.007	None	16.0	Value of Δf^2 for limiting integral control
E_{12}	5.0	sec	12905.55	Parking orbit equation lockout
E_{13}	550.0	$(ft/sec^2)^2$	270400.0	Acceleration value for switching to second-burn equations
E_{14}	0.28×10^8	$(ft/sec)^2$	$0.27487791 \times 10^{10}$	Energy-to-be-gained to enter second MECO cutoff computation

Table A-2. Equation Switching Constants (Contd)

CONSTANT	VALUE	UNITS	SCALE FACTOR	DEFINITION
E_{15}	125.0	sec	12905.55	Second MECO time backup
E_{16}	60.0	sec	12905.55	Time from second MECO for computation of reorient reference vector
E_{17}	10.0	None	0.262144×10^{6}	Iteration counter for $\|\bar{f}\|$ calculation in postinjection phase
E_{18}	88.7	sec	12905.55	Time to begin telemetry calibration in postinjection phase
E_{19}	3.48	sec	12905.55	Time to end telemetry calibration in postinjection phase

Table A-3. Initialization Constants

CON-STANT	VALUE	UNITS	SCALE FACTOR	DEFINITION
I_1	-32.2	ft/sec^2	65.0	Initial value of g^*_{wi-1}
I_2	36.0	ft/sec^2	520.0	Initial value of $\|\bar{a}_T\|$
I_3	1340.0	ft/sec	104857.6	Initial value of Y
I_4	25500.0	ft/sec	52428.8	Initial value of v_{rt}
I_5	18700.0	ft/sec	52428.8	Initial value of $\|\bar{f}\|$
I_6	20909816.0	ft	42288908.8	Initial value of r_{gwi-1}
I_7	-0.65625650×10^9	$(ft/sec)^2$	$0.26487791 \times 10^{10}$	First-burn MECO cutoff energy
I_8	1.5	None	0.262144×10^6	Iteration counter for $\|\bar{f}\|$ calculation in sustainer and Centaur phases
I_9	0.0161	sec	100.82461	First-burn MECO time bias

Table A-4. Launch Day Dependent Constants for 26 April 1966

CONSTANT	VALUE	UNITS	SCALE FACTOR	DEFINITION
J_1	0.	sec	0.51622205+05	Constant for elapsed-time-into-launch-window equation
J_2	0.12166561+04	ft/sec	0.52428799+05	Initial v_{gu}
J_3	0.56733435+03	ft/sec	0.52428799+05	Initial v_{gv}
J_4	0.24823368+05	ft	0.42288908+08	Initial r_{gu}
J_5	-0.53233884+05	ft	0.42288908+08	Initial r_{gv}
J_6	-0.87688597+00	None	2.0	Constants for target vector component 1_{au}
J_7	0.	sec^{-1}	0.15497208-03	
J_8	0.	sec^{-2}	0.12008172-07	
J_9	0.	sec^{-3}	0.93046569-12	
J_{10}	0.	sec^{-4}	0.72098099-16	
J_{11}	-0.19796295+00	None	2.0	Constants for target vector component 1_{av}
J_{12}	0.	sec^{-1}	0.15497208-03	
J_{13}	0.	sec^{-2}	0.12008172-07	
J_{14}	0.	sec^{-3}	0.93046569-12	
J_{15}	0.	sec^{-4}	0.72098099-16	
J_{16}	0.43804292+00	None	2.0	Constants for target vector component 1_{aw}
J_{17}	0.	sec^{-1}	0.15497208-03	
J_{18}	0.	sec^{-2}	0.12008172-07	
J_{19}	0.	sec^{-3}	0.93046569-12	
J_{20}	0.	sec^{-4}	0.72098099-16	

Table A-4. Launch Day Dependent Constants for 26 April 1966, Contd

CONSTANT	VALUE	UNITS	SCALE FACTOR	DEFINITION
J_{21}	-0.12056655+08	ft^2/sec^2	0.27487791+10	Constants for nominal injection vis-viva energy
J_{22}	0.	ft^2/sec^3	0.21299200+06	
J_{23}	0.	ft^2/sec^4	0.16503906+02	
J_{24}	0.	ft^2/sec^5	0.12788223-02	
J_{25}	0.	ft^2/sec^6	0.99090873-07	
J_{26}	0.26024110-00	None	2.0	Constants for nominal injection sin θ
J_{27}	0.	sec^{-1}	0.15497208-03	
J_{28}	0.	sec^{-2}	0.12008172-07	
J_{29}	0.13671909+04	ft/sec	0.52428799+05	Constants for v_{rr} C_2 coefficient
J_{30}	0.	ft/sec^2	0.40624999+01	
J_{31}	0.	ft/sec^3	0.31478703-03	
J_{32}	0.14560000+04	sec	0.12905550+05	Constants for parking orbit backup
J_{33}	0.	None	1.0	
J_{34}	0.44770757-22	sec^5/ft^5	0.16155871-21	Constants for pitch profile gain, G_r first Centaur burn
J_{35}	-0.25085266-27	sec^5/ft^6	0.97801130-27	
J_{36}	0.98563999+02	sec	0.12905550+05	Constant for $\bar{f}$* vector during coast phase. Also used as time test constant
J_{37}	-0.99936301+00	None	2.0	Constants for the parking orbit termination parameter ϕ
J_{38}	0.35687078-01	None	1.0	

Table A-4. Launch Day Dependent Constants for 26 April 1966, Contd

CONSTANT	VALUE	UNITS	SCALE FACTOR	DEFINITION
J_{39}	0.21539441+08	ft	0.42288908+08	Constant for nominal injection r_m
J_{40}	0.24999999-14	sec^3/ft^3	0.69388937-14	Constant for pitch profile gain, G_r second burn

Table A-5. Equation Input Constants

CONSTANT	VALUE	UNITS	SCALE FACTOR	DEFINITION
K_1	$-0.11023109 \times 10^{-3}$	sec^{-1}	$0.12397765 \times 10^{-2}$	Required velocity polynominal coefficients
K_2	0	sec^{-1}	$0.12397765 \times 10^{-2}$	
K_3	0	sec/ft^2	$0.36082248 \times 10^{-11}$	
K_4	18518.358	ft/sec	26214.4	
K_5	0	ft/sec	13107.2	
K_6	0	sec/ft	$0.19073486 \times 10^{-4}$	
K_7	$0.14076539 \times 10^{17}$	ft^3/sec^2	$0.11624286 \times 10^{18}$	Earth gravitational constant
K_8	$0.88888888 \times 10^{-5}$	sec^2/ft^2	$0.11920928 \times 10^{-4}$	Modified yaw gain constant in alternate v_{rn} logic
K_9	0.8×10^{-8}	sec^2/ft^2	$0.23283064 \times 10^{-7}$	Yaw gain constant
K_{10}	0.35	None	1.0	f*u in booster phase (1)
K_{11}	0.15	None	1.0	f*v in booster phase (1)
K_{12}	0.15	None	1.0	f*w in booster phase (1)
K_{13}	26.5	ft/sec^2	520.0	Initialization of $\lvert\bar{a}_T\rvert$ for Centaur first burn
K_{14}	0.21102566×10^8	ft	42288908.8	Centaur first-burn altitude control polynominal coefficients
K_{15}	0.37075656×10^4	ft/sec	26214.4	

(1) for ground checkout purposes only

Table A-5. Equation Input Constants (Contd)

CONSTANT	VALUE	UNITS	SCALE FACTOR	DEFINITION
K_{16}	$-0.10443842 \times 10^{2}$	ft/sec^{2}	16.25	Centaur first-burn altitude control polynominal coefficients
K_{17}	0.8827185×10^{-2}	ft/sec^{3}	$0.10073184 \times 10^{-1}$	
K_{18}	5.3	ft/sec	52428.8	Centaur first-burn G_r bias
K_{19}	0.15	sec^{-1}	1.2695312	Integral gain constant
K_{20}	0.409259	None	0.5	Steering gain constant
K_{21}	0.0132	sec	100.82461	Second MECO time bias
K_{22}	10000.0	ft/sec	52428.8	Initialization of $\lvert\bar{f}\rvert$ for second burn
K_{23}	69.5	ft/sec^{2}	520.0	Initialization of $\lvert\bar{a}_T\rvert$ for second burn
K_{24}	36000.0	ft/sec	52428.8	Initialization of $\lvert\bar{f}\rvert$ for postinjection phase

N6723262

An analysis based on telemetered digital computer and pulse data, of the guidance equations and guidance hardware is presented. All of the first-burn and coast guidance objectives are reported fulfilled. ~~At second mission event sequence the G2 engine ignited briefly for a brief for a brief period~~ but the second MES was not successful because of H_2O_2 depletion. Among the conclusions are: (1) The guidance computer operated flawlessly until the end of telemetry coverage. (2)